DICAM

Dipartimento di ingegneria civile, ambientale e dei materiali

**Dottorato di Ricerca in
Ingegneria Civile ed Ambientale
Ciclo XXVI**

Settore Concorsuale di afferenza: 08/B1 Geotecnica
Settore Scientifico disciplinare: ICAR/07 Geotecnica

A New Prediction Model for Slope Stability Analysis

Presentata da Azadeh Rashed

Coordinatore Dottorato   **Relatore**
Prof. Alberto Lamberti   **Prof. Guido Gottardi**

                                              Correlatore
                                              Eng. Amir Hossein Alavi

ACKNOWLEDGEMENTS

ABSTRACT

The instability of river bank can result in considerable human and land losses. The Po river is the most important in Italy, characterized by main banks of significant and constantly increasing height. This study presents multilayer perceptron of artificial neural network (ANN) to construct prediction models for the stability analysis of river banks along the Po River, under various river and groundwater boundary conditions. For this aim, a number of networks of threshold logic unit are tested using different combinations of the input parameters. Factor of safety (FS), as an index of slope stability, is formulated in terms of several influencing geometrical and geotechnical parameters. In order to obtain a comprehensive geotechnical database, several cone penetration tests from the study site have been interpreted. The proposed models are developed upon stability analyses using finite element code over different representative sections of river embankments. For the validity verification, the ANN models are employed to predict the FS values of a part of the database beyond the calibration data domain. The results indicate that the proposed ANN models are effective tools for evaluating the slope stability. The ANN models notably outperform the derived multiple linear regression models.

Table of Contents

CHAPTER1 INTRODUCTION

CHAPTER2 SLOPE STABILITY EVALUATION

CHAPTER3 ARTIFICIAL NEURAL NETWORKS

CHAPTER4 STABILITY EVALUATION OF PO RIVER BANKS

CHAPTER5 PROPOSED NEURAL NETWORK MODEL FOR SLOPE STABILITY ANALYSIS

CHAPTER6 CONCLUSION

List of Figures

List of Tables

CHAPTER 1
INTRODUCTION

1- 1 Introduction

Slope stability has been a subject of continued concern because of tremendous loss of properties and infrastructure caused annually in many places in the word (Shioi and Sutoh, 1999; Zhang, 2001). In construction areas, instability may result due to rainfall, increase in groundwater table and change in stress conditions. Similarly, slopes that have been stable for many years may suddenly fail due to changes in geometry, external forces and loss of shear strength (Abramson et al. 2002).

Slope failures, also referred to as slides or landslides, whether sudden or gradual, are due to overstress of the slope or foundation materials with respect to their available strength (Morgenstem 1963; Davis, 1968; Ching and Fredlund, I983; Abramson, 1996; Dai et al., 2000). Overstresses may occur due to the following:

1) factors causing an increase in shear stress (e.g., external loads, steepening of slope, undercutting of a slope at the toe. sudden draw down, earthquakes);

2) factors causing a decrease in shear strength (e.g., liquefaction triggered by shock or dynamic forces, saturation of a slope particularly in desiccated soils, other factors that increase excess pore water pressure);

3) hydrodynamic forces (such as earthquake-induced waves, seepage forces);

4) hydrostatic forces (such as tension cracks filled with water in fissured clays or desiccated clays, artesian pressures in filled aquifers).

Due to numerous factors affecting slope failures, slope stability analyses have always been a difficult and complex task in geotechnical engineering and geomechanics (Cousins, 1978; Leshchinsky et al., 1985; Wakai and Ugai, 1999).

The majority of slope stability analyses performed in practice still use traditioanal limit equilibrium approaches involving methods of slices that have been remained essentially unchanged for decades. The finite element method in conjunction with elastic-perfectly plastic (Mohr-Coulomb) stress strain model represents a powerful alternative approach for slope stability analysis which is accurate, versatile and requires fewer a priori assumptions, especially regarding to failure mechanism. Slope failure in the finite element model occures "naturally" through the zones in which the shear strength of the soil is insufficient to resist the shear stresses.

Since many factors are involved in modeling slope stability, physics-based models can have difficulties in representing real-life situations and in considering such important factors as slope geometry and soil properties affecting the stability of slopes (Bishop, 1971, Jiao et al.. 2000). The neural network approach can be a useful modeling tool in such situations. Among important attributes, neural network models are based on laboratory and/or field data and thus it is easier to include the factors affecting slope stability in such models. Because artificial neural network models have learning capability that physics-based models do not have, they can model slopes with a reasonable accuracy even when some data pertaining to geometric and/or soil properties are unavailable.

1-2 Scope and Objective of the Study

In this study, artificial neural network modeling approach is used for analyses of slopes. For developing the neural network model as adopted in this study, stability analyses using finite element code over different representative sections of Po river embankments contributed to the database. Po River is the most important in Italy.

In order to obtain a comprehensive geotechnical database, several cone penetration tests with the measurement of pore water pressure (CPTu) from the study site have

been interpreted with the use of a self-developed CPTu interpreting program based on most reliable and recent empirical an semi- empirical correlations.

The specific Steps in order to fulfill this study include the following:

(i) Develop a program in order to interpret cone penetration tests with the measurement of pore water pressure (CPTu);

(ii) Interpreting of 220 CPTu tests to obtain a comprehensive geotechnical database.

(iii) Stability analysis of 77 Po river banks with the use of FE based program (Plaxis2D version 2012).

(iv) Develop an artificial neural network-based model for analysis of slope stability with the contribution of FE analysis results;

(v) Compare the performance of ANN model with a developed multiple linear regression models.

1- 3 Format of the Dissertation

Presentation of this thesis has been organized in several Chapters and Appendices. A brief description is given here. The introduction to slope stability problems and a detailed literature review of the methods of slope stability analysis is presented in Chapter2, The review focuses on the limit equilibrium (LE) and finite element(FE) principles in FOS determination. Moreover, most common LE methods are discussed with highlights on their fundamental differences and limitations in practical applications.

Finally, the chapter ends with introducing brief working principles of FE computer software codes (PLAXIS2D) that are applied in the present study.

Chapter 3 describes artificial neural networks and their application in geotechnical engineering. Soil stratigraphy with the use of CPTu tests on Po riverbanks and

their FE analysis is presented in chapter4. Moreover a description of the study site and one of the most reliable geotechnical in-situ test (CPTu) is concluded. Chapter5 presents the proposed neural network method for modeling slope stability. The proposed models are developed upon stability analyses using finite element code over different representative sections of river embankments. Finally, in Chapter6 summary and conclusions of this study are presented and, recommendations for further studies are discussed.

CHAPTER2
SLOPE STABILITY EVALUATION

2- 1 Introduction

Slope stability analysis is an important area in geotechnical engineering. A detailed review of equilibrium methods of slope stability analysis is presented by Duncan (Duncan, 1996). These methods, in general, require the soil mass to be divided into slices. The directions of the forces acting on each slice in the slope are assumed. This assumption is a key role in distinguishing one limit equilibrium method from another.

Limit equilibrium methods require a continuous surface passes the soil mass. This surface is essential in calculating the minimum factor of safety (FOS) against sliding or shear failure. Before the calculation of slope stability in these methods, some assumptions, for example, the side forces and their directions, have to be given out artificially in order to build the equations of equilibrium.

In the past decades finite element method has been increasingly used in slope stability analysis. The advantage of a finite element approach in the analysis of slope stability problems over traditional limit equilibrium methods is that no assumption needs to be made in advance about the shape or location of the failure surface, slice side forces and their directions. The method can be applied with complex slope configurations and soil deposits in two or three dimensions to model virtually all types of mechanisms. General soil material models that include Mohr-Coulomb and numerous others can be employed. The equilibrium stresses, strains, and the associated shear strengths in the soil mass can be computed very accurately. The critical failure mechanism developed can be extremely general and need not be simple circular or logarithmic spiral arcs. The method can be extended

to account for seepage induced failures, brittle soil behaviors, random field soil properties, and engineering interventions such as geo-textiles, soil nailing, drains and retaining walls. This method can give information about the deformations at working stress levels and is able to monitor progressive failure including overall shear failure (Griffiths, 1999).

2- 2 Limit Equilibrium Methods

 Limit equilibrium methods are still currently most used for slopes stability studies. These methods consist in cutting the slope into fine slices so that their base can be comparable with a straight line then to write the equilibrium equations (equilibrium of the forces and/or moments). According to the assumptions made on the efforts between the slices and the equilibrium equations considered, many alternatives were proposed (Table 2-1). They give in most cases rather close results. The differences between the values of the safety factor obtained with the various methods are generally lower than 6% (Duncan, 1996).

Table 2- 1 The main limit equilibrium methods (Duncan et al, 1987)

Methods	Equilibrium conditions satisfied	Slip surface	Use
Ordinary Method of Slices (Fellenius, 1927)	Moment equilibrium about center of circle	Circulaire slip surface	Applicable to non-homogeneous slopes and c-ø soils where slip surface can be approximated by a circle. Very convenient for hand calculations. Inaccurate for effective stress analyses with high pore water pressures.
Bishop's Modified Method (Bishop, 1955)	Vertical equilibrium and overall moment equilibrium	Circular	Applicable to non-homogeneous slopes and c-ø soils where slip surface can be approximated by a circle. More accurate than Ordinary Method of slices, especially for analyses with high pore water pressures. Calculations feasible by hand or spreadsheet.
Janbu's Generalized Procedure of Slices (Janbu, 1968)	Force equilibrium (vertical and horizontal)	Any shape	Applicable to non-circular slip surfaces. Also for shallow, long planar failure surfaces that are not parallel to the ground surface.
Morgenstern & Price's Method (Morgenstern & Price's, 1965)	All conditions of equilibrium	Any shape	An accurate procedure applicable to virtually all slope geometries and soil profiles. Rigorous, well established complete equilibrium procedure.
Spencer's Method (Spencer, 1967)	All conditions of equilibrium	Any shape	An accurate procedure applicable to virtually all slope geometries and soil profiles. The simplest complete equilibrium procedure for computing factor of safety.

All limit equilibrium methods utilise the Mohr-Coulomb expression to determine the shear strength (τ_f) along the sliding surface. The shear stress at which a soil fails in shear is defined as the shear strength of the soil. According to Janbu (1973), a state of limit equilibrium exists when the mobilised shear stress (τ) is expressed as a fraction of the shear strength. Nash (1987) says, "At the moment of failure, the shear strength is fully mobilised along the failure surface when the critical state conditions are reached". The shear strength is usually expressed by the Mohr-Coulomb linear relationship, where the τ_f and τ are defined by:

Shear strength (available): $\tau_f = c' + \sigma' \tan \emptyset'$ or $(a + \sigma') \tan \emptyset'$ (2-1)

Shear stress (mobilised): $\tau = \dfrac{\tau_f}{F} = \dfrac{c' + \sigma' \tan \emptyset'}{F}$ (2-2)

Where, a, c´ and $\emptyset'$ = attraction, cohesion and friction angle respectively in effective stress terms, and F = factor of safety (FOS).

The available shear strength depends on the type of soil and the effective normal stress, whereas the mobilized shear stress depends on the external forces acting on the soil mass. This defines the FOS as a ratio of the τ_f to τ in a limit equilibrium analysis (Janbu 1954), as defined in Equation 2-2.

However, the FOS can be defined in three ways: Limit equilibrium, force equilibrium and moment equilibrium (Abramson et al. 2002). These definitions are given in Figure 2-1. As explained above, the first definition is based on the shear strength, which can be obtained in two ways: A total stress approach (su-analysis) and an effective stress approach (a-φ −analysis). The type of strength consideration depends on the soil type, the loading conditions and the time elapsed after excavation. The total stress strength is used for short–term conditions in clayey soils, whereas the effective stress strength is used in long-term conditions in all kinds of soils, or any conditions where the pore pressure is known (Janbu 1973).

The second and third definitions are based on force equilibrium and movement equilibrium conditions for resisting and driving force and moment components respectively.
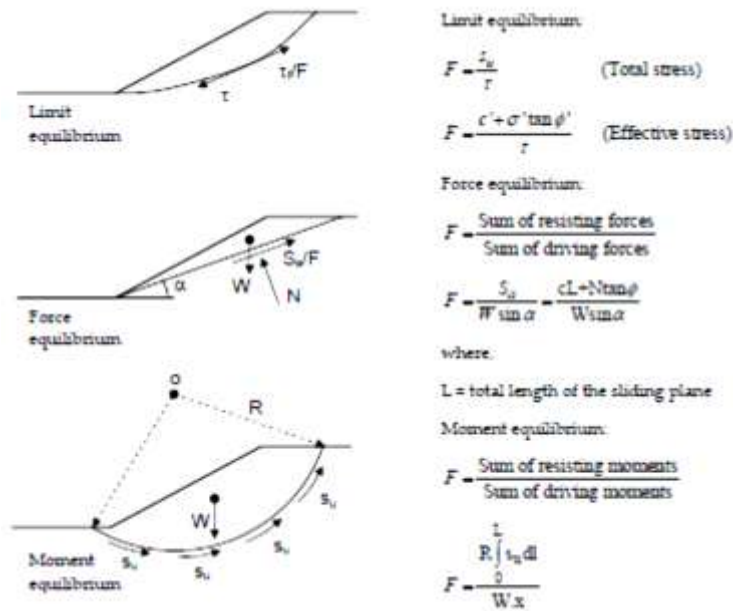
Figure 2- 1 Various definitions of the factor of safety (FOS) (Abramson et al. 2002)

The last two definitions may sometimes be confusing while defining the terms, whether the force or moment components are contributing on resisting or driving sides. The reason can be explained with simple examples. The support force component along the sliding surface can be considered on the resisting side as a positive contribution, since it increases resistance capacity against the movement. At the same time, this component can also be considered on driving side as negative contribution, since it decreases the driving tendency. Similarly, the moments from the self weight of slices located at the toe are sometimes resisting and thus, considered either on the resisting side as positive contribution or on the driving side as negative contribution. These two different considerations result in different FOS. But this is not a case in the first definition.

2-2- 1 The Ordinary method

The Ordinary method satisfies the moment equilibrium for a circular slip surface, but neglects both the interslice normal and shear forces. The advantage of this method is its simplicity in solving the FOS, since the equation does not require an iteration process. The forces considered in ordinary method are shown in figure 2-2. The FOS is based on moment equilibrium and computed by (Abramson et al. 2002, Nash 1987):

$$F_m = \frac{\Sigma(c\,'l + N\,'\tan\emptyset\,')}{\Sigma W \sin\alpha} \tag{2-3}$$

$$N\,' = (W\cos\alpha - ul) \tag{2-4}$$

Where, u = pore pressure, l = slice base length and α = inclination of slip surface at the middle of slice.
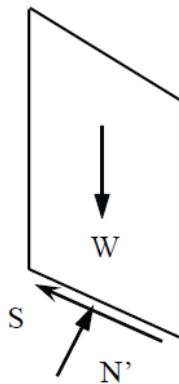
Figure 2- 2 The forces considered in ordinary method

2-2- 2 Bishop'S Simplified Method of Slices

Bishop's method of slices (1955) is useful if a slope consists of several types of soil with different values of c and $\emptyset$ and if the pore pressures u in the slope are known or can be estimated. Figure 2-3 gives a section of an earth dam having a sloping

surface *AB.* The soil mass above the failure surface is divided into a number of slices.

Consider for analysis a single slice *abed* [Figure 2 -3 (a)] which is drawn to a larger scale in Figure 2 -3 (b). The forces acting on this slice are

W = weight of the slice

N = total normal force on the failure surface *cd*

U = pore water pressure = *ul* on the failure surface *cd*

FR = shear resistance acting on the base of the slice

E1, E2 = normal forces on the vertical faces *be* and *ad*

T1, T2 = shear forces on the vertical faces *be* and *ad*

θ = the inclination of the failure surface *cd* to the horizontal

The system is statically indeterminate. An approximate solution may be obtained by assuming that the resultant of £, and *T^* is equal to that of *E2* and *T2,* and their lines of action coincide.

(a)   (b)
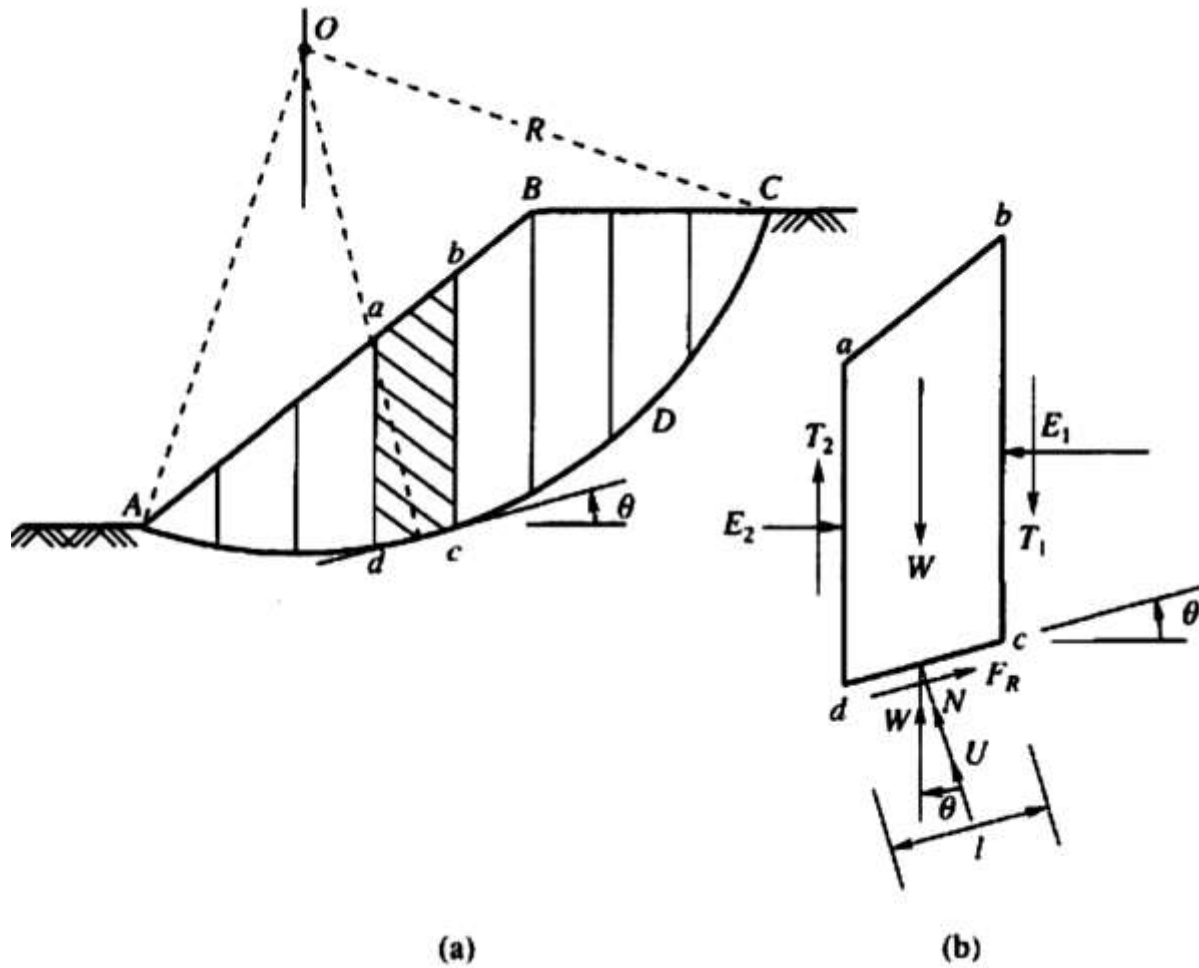
Figure 2- 3 Bishop's simplified method of analysis

The factor of safety Fs is then given as

$$F_s = \frac{\Sigma\{c'l\cos\theta+[(W-U\cos\theta)+\Delta T]\tan\phi'\}\frac{1}{m_\theta}}{\Sigma W\sin\theta}$$ (2-5)

Where

$$m_\theta = \cos\theta + \frac{\tan\phi'\sin\theta}{F_s}$$ (2-6)

The value of Fs may then be computed by first assuming an arbitrary value for Fs. The value of Fs may then be calculated by making use of equation 2-5. If the calculated value of Fs differs appreciably from the assumed value, a second trial is

made and the computation is repeated. Figure 2 -4 developed by Janbu et al. (1957) helps to simplify the computation procedure.

Note: θ is + when slope of failure arc is in the same quadrant as ground slope.

$m_\theta = \cos \theta + (\sin \theta \tan \phi')/F_s$
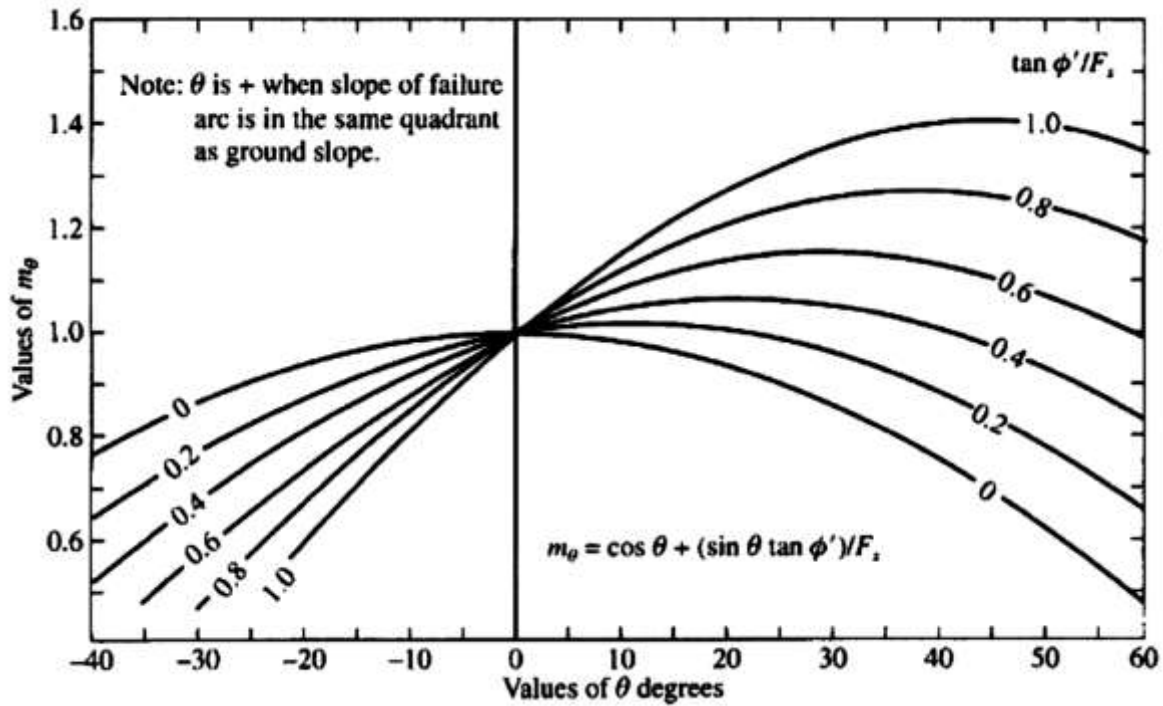
Figure 2- 4 Values of m_θ (Janbu et al., 1957)

In summary, Bishop's simplified method satisfies moment equilibrium for FOS, satisfies vertical force equilibrium for N, considers interslice normal force, more common in practice, and applies mostly for circular shear surfaces. The forces considered in Bishop's simplified method are shown in figure 2-5.
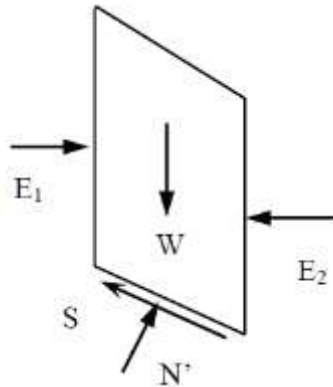
Figure 2- 5 forces considered in Bishop's simplified method

2-2- 3 Janbu's generalised method

Janbu's generalised method or Janbu's generalised procedure of slices (Janbu 1973) considers both interslice forces and assumes a line of thrust to determine a relationship for interslice forces. As a result, the FOS becomes a complex function with both interslice forces (Nash 1987):

$$F_f = \frac{\sum[\{c'l+(N-ul)\tan\emptyset'\}\sec\alpha]}{\sum\{W-(T_2-T_1)\}\tan\alpha+\sum(E_2-E_1)} \tag{2-7}$$

Similarly, the total base normal force (N) becomes a function of the interslice shear forces (T) as:

$$N = \frac{1}{m_\alpha}\left\{W-(T_2-T_1)-\frac{1}{F}(c'l-u\tan\emptyset')\sin\alpha\right\} \tag{2-8}$$

This is the first method that satisfies both force and moment equilibrium. The moment equilibrium for the total sliding mass is explicitly satisfied by considering an infinitesimal slice width (dx) and taking moments about the mid point of the slice base (Janbu 1957, 1973). The infinitesimal slice width was introduced to avoid the confusion about the point of application of base normal force. This equilibrium condition in fact gives the relationship between the interslice forces (E and T) as:

$$T = \tan\alpha_t E - \frac{dE}{dx}h_t \tag{2-9}$$

Where, $tan\alpha_t$ = slope of the line of thrust, and h_t = height from the mid point of the slice base to dE.

The interslice force relationship obtained in equation 2-9 is the same as Janbu first established, except for the interslice shear force direction, which is assumed here counter-clockwise for a slide occurring from left to right as shown in figure 2-6.

The last term in equation 2-9 cannot be ignored because of the gradient of interslice normal force with respect to distance.

The line of thrust follows the centroid of the earth pressure (Janbu 1973, Nash 1987). However, for statically determinate solutions, the actual location is searched for by an iteration procedure until the total equilibrium is satisfied (Abramson et al. 2002). Since the overall force equilibrium is satisfied by the interslice forces, the moment equilibrium automatically fulfils for the sliding mass (Nash 1987).
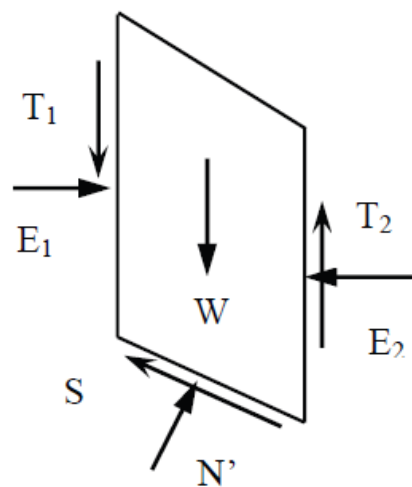
Figure 2- 6 forces considered in Janbu's generalised method

2-2- 4 Morgenstern-Price method

This is perhaps the best known and most widely used method developed for analyzing generalized failure surfaces. The method was initially described by Morgenstem and Price (1965).The Morgenstern- Price method also satisfies both force and moment equilibriums and the overall problem is made determinate by assuming a functional relationship between the interslice shear force and the interslice normal force. According to Morgenstem and Price (1965), the interslice force inclination can vary with an arbitrary function (f(x)) as:

$$T = f(x). \lambda. E \hspace{6cm} (2\text{-}10)$$

where,

f(x) = interslice force function that varies continuously along the slip surface

and λ = scale factor of the assumed function.

The method suggests assuming any type of force function, for example half-sine, trapezoidal or user defined. The relationships for the base normal force (N) and interslice forces (E, T) are the same as given in Janbu's generalised method. For a given force function, the interslice forces are computed by iteration procedure until, F_f is equals to F_m in equations (2-11) and (2-12) (Nash 1987).

$$F_f = \frac{\sum[\{c'l+(N-ul)\tan\emptyset'\}\sec\alpha]}{\sum\{W-(T_2-T_1)\}\tan\alpha+\sum(E_2-E_1)} \qquad (2\text{-}11)$$

$$F_m = \frac{\sum(c'l+(N-ul)\tan\emptyset')}{\sum W\sin\alpha} \qquad (2\text{-}12)$$
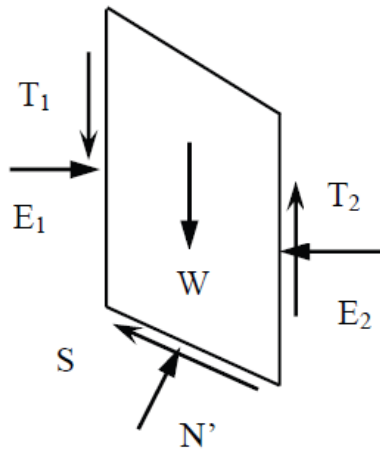
Figure 2- 7 Forces considered in Morgenstern-Price method

The Morgenstem Price method is fairly widely used and accepted for general analysis of non-circular failure surfaces and its results have been verified in several

comparative studies; but acceptability of solutions should always be checked (Costa and Thomas. 1984; Abramson, 1996).

2-2- 5 Spencer's method

Spencer's method is the same as Morgenstem Price method except the assumption made for interslice forces. A constant inclination is assumed for interslice forces and the FOS is computed for both equilibriums (Spencer 1967). According to this method, the interslice shear force is related to:

$$T = E \tan \theta \tag{2-13}$$

In summary, Spencer's method, considers both interslice forces, assumes a constant interslice force function, satisfies both moment and force equilibrium, and computes FOS for force and moment equilibrium.

The forces considered are shown in figure 2-8.
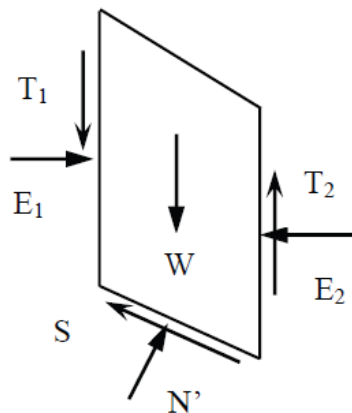
Figure 2- 8 Forces considered in Spencer's method

2- 3 Finite Element Method

The finite element method (FEM) represents a powerful alternative approach for slope stability analysis. This method is accurate, versatile, and requires fewer a priori assumptions, especially regarding the failure mechanism. The FEM is very

powerful in solving problems with irregular boundaries and complex variation of potential and flow lines (Zaman et al., 2000). The region to be analyzed is divided into elem ents which are joined at nodes. The unknown displacements at each node may be computed and from these the strain and stress fields within the body may be found.

The main advantages of the FE approach over traditional limit equilibrium methods for slope stability analysis are that no assumption needs to be made in advance about the shape or location of the failure surface, slice side forces and their directions and the slip surface could be of any shape (Chollada, 2013). General soil material models that include Mohr-Coulomb and numerous others can be employed.

Limit equilibrium methods only give an estimate of FS with no information on deformation of the slope. In numerical analysis, failure occurs "Naturally" which evolve during the calculation in a way that is representative of the natural evolution of the physical failure plane in the slope (Wyllie and Mah, 2004).

2- 4 Computer Codes used for stability analysis

Slope stability analyses today can be performed by using various computer based geotechnical software. Software utilizing LE formulations has been used for many years. Similarly, finite element (FE) software, based on constitutive laws and appropriate soil models, has drawn growing interest both of researchers and of professionals. Today, both LE and FE based software are commonly used in geotechnical computations. A brief introduction and working principles of the software that are used in this study is briefly introduced in the following sections.

2-4- 1 SLOPE/W software

SLOPE/W, developed by GEO-SLOPE International Canada, is used for slope stability analysis.

This software is based on the theories and principles of the LE methods discussed in the previous sections. In this study, SLOPE/W has been applied separately and together with SEEP/W, other software program, which computes the pore pressure distributions, based on finite elements mesh and groundwater seepage analyses. Finally, the pore pressure distributions were coupled with slope stability analysis and FOS was determined. The software SLOPE/W computes FOS for various shear surfaces, for example circular, non-circular and user-defined surfaces (SLOPE/W 2002, Krahn 2004). However, only the circular SS is automatically searched.

2-4- 2 The SLIDE software

SLIDE software, developed by Rocscience Inc Toronto Canada, is also used for slope stability analysis for soil and rock slopes. The software is also 2D-LE based computer program, which can be applied to evaluate the stability for circular or non-circular failure surfaces (SLIDE 2003).

In fact, SLIDE is found similar to the SLOPE/W though there are few additional features, for example groundwater analysis and back analysis for support forces.

Modelling in SLIDE for the study was possible for external loading, groundwater and forces, like surcharge and from pseudo-static earthquakes. The circular critical slip surface was located automatically and the corresponding FOS was computed by the software in the similar way as in SLOPE/W.

2-4- 3 The PLAXIS software

PLAXIS is a finite element code for soil and rock analyses (PLAXIS 2012), developed by PLAXIS BV in cooperation with several universities including DUT in the Netherlands and NTNU in Norway. The computer program is applicable to many geotechnical problems, including stability analyses and steady-state groundwater flow calculations. This software contains several FE models and four main sub-routines. These routines are inputs, calculations, outputs and curve plots. The FOS versus displacement is plotted from the curve plots sub-routine.

The FE code Plaxis2D version 2012 in conjunction with an elastic-perfectly plastic (Mohr-Coulomb) stress strain model has been used in this study. Material properties including shear strength parameters were defined for each soil layer. A plain strain model of 15 noded triangular elements was used to generate the finite element mesh. Similarly, pore pressure distributions were generated based on phreatic level with and without corrections and the steady-state groundwater calculation.

The Mohr-Coulomb failure criterion is currently the most widely used method for soil in practical applications (El-Naggar, 2010). The Mohr–Coulomb model is a linearly elastic and perfectly plastic constitutive model. The parameters needed for the Mohr–Coulomb model are the Young's modulus (E) and Poisson's ratio (ν) for the elastic strain component of the soil behavior. The effective strength parameters cohesion (c'), and friction angle (φ'), as well as the dilatancy angle (ψ) are needed for the plastic strain component of the soil behavior.

2-4-3- 1 Computation of FOS

FOS was computed by using the 'c-φ reduction' procedure. According to PLAXIS2D version 2012, this approach involves in successively reducing the soil

strength parameters c' and tanφ' until the failure occurs. The strength parameters are automatically reduced until the final calculation step results in a fully developed failure mechanism. Further, Nordal and Glaamen (2004) say, "By lowering the strength incrementally, a soil body is identified to fail after a certain strength reduction". In this way, PLAXIS computes the FOS as the ratio of the available shear strength to the strength at failure by summing up the incremental multiplier (Msf) as defined by:

FOS= Value of $\sum M_{sf}$ at failure $= \dfrac{\tan \emptyset_{input}}{\tan \emptyset_{reduced}} = \dfrac{c_{input}}{c_{reduced}}$ (2-14)

Chapter 3
Artificial Neural Network

3-1 Introduction

Artificial neural networks (ANNs) are a form of artificial intelligence which attempt to mimic the function of the human brain and nervous system. ANNs learn from data examples presented to them in order to capture the subtle functional relationships among the data even if the underlying relationships are unknown or the physical meaning is difficult to explain. This is in contrast to most traditional empirical and statistical methods, which need prior knowledge about the nature of the relationships among the data. ANNs are thus well suited to modeling the complex behavior of most geotechnical engineering materials which, by their very nature, exhibit extreme variability. This modeling capability, as well as the ability to learn from experience, have given ANNs superiority over most traditional modeling methods since there is no need for making assumptions about what the underlying rules that govern the problem in hand could be.

3-2 Artificial Neuron Model and Network Architecture

The neuron model and the architecture of a neural network describe how a network transforms its input into an output. This transformation can be viewed as a computation. The model and the architecture each place limitations on what a particular neural network can compute (Hertz et al. 1991). The way a network computes its output must be understood before training methods for the network can be explained.

3-2- 1 Artificial Neuron Model

A single artificial neuron with R inputs is shown in Figure 4-1. Here the input vector p is represented by the solid dark vertical bar at the left. The dimensions of p are shown below the symbol p in the figure as $Rx\ l$. Thus, p is a column n vector of R input values. These inputs go to the row vector w. which is of size R.
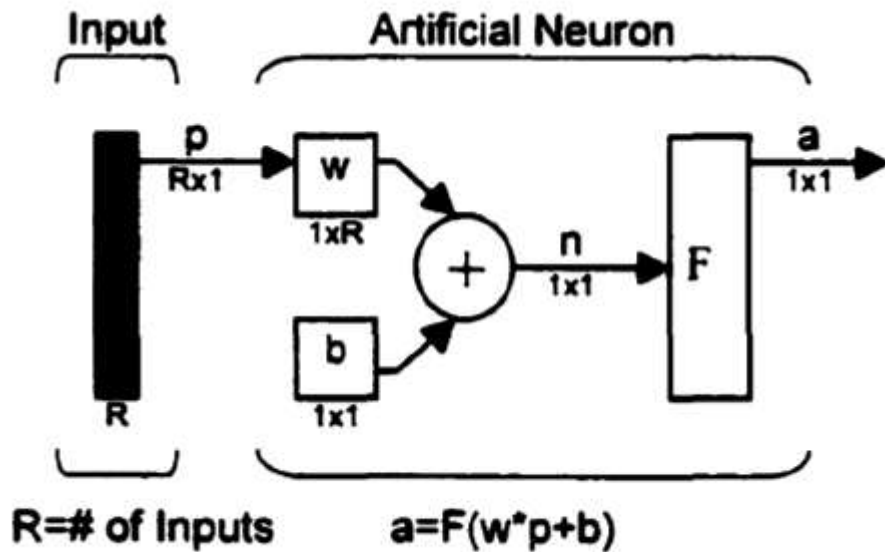
Figure 3- 1 Artificial Neuron Model (McCullock and Pitts, 1943)

As shown in Figure 4-1, the net input to the transfer function F is n, the sum of the bias b and the product $w\times p$. This sum is passed to the transfer function F to get the neuron's output a. which in this case is a scalar. If we have more than one neuron, the network output will be a vector. The row vector w and the column vector p are shown below.

$$w = [w(1.1)w(1.2)...w(1.R)]$$ (4-1)

$$p = [p(1)p(2)...p(R\ )]^T$$ (4-2)

A layer of a network is defined in the figure shown above. A layer includes the combination of the weights, the multiplication and summing operation, the bias *b*. and the transfer function *F*. The input vector, *p*. will not be called a layer.

The transfer function *F* can take different shapes depending on different problems. Two of the most commonly used functions are shown below. The linear transfer function, as shown in Figure 4-2. can be used as a linear approximator (Widrow and Hoff. 1960: Hertz e tal.. 1991).
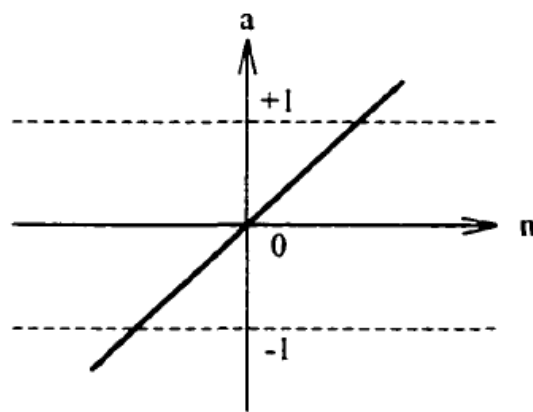
Figure 3- 2 Linear Transfer Function (Widrow and Hoff, 1960)

The sigmoid transfer functions, as shown in Figure 4-3. takes the input and transforms the output into the range -1 to +1. This transfer function is commonly used in multiple-layer networks, in part because it is differentiable (McClelland and Rumelhart. 1986; Demuth and Beale, 1995).
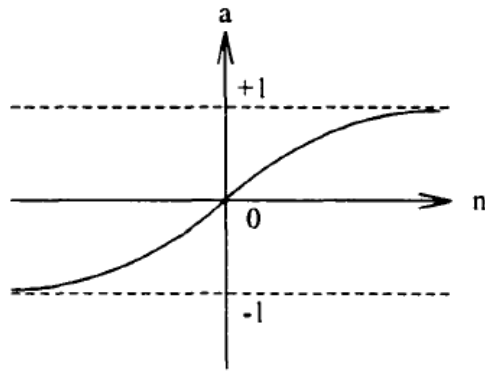
Figure 3- 3 Sigmoid Transfer Function (McClelland and Rumelhart. 1986)

3-2- 2 Neural Network Architecture

Two or more of the neurons shown in Figure 4-1 may be combined into a layer, and a particular network might contain one or more such layers.

3-2-2- 1 Single-layer Network

A single-layer network with *R* inputs and *S* neurons is shown below. Here *p* is an input vector of length *R*. w is a matrix (SxR) as shown below, and *a* and *b* are vectors of length *S*. As defined previously, the neuron layer includes the weight matrix, the multiplication operations, the bias vector *b,* the sum , and the transfer function boxes.
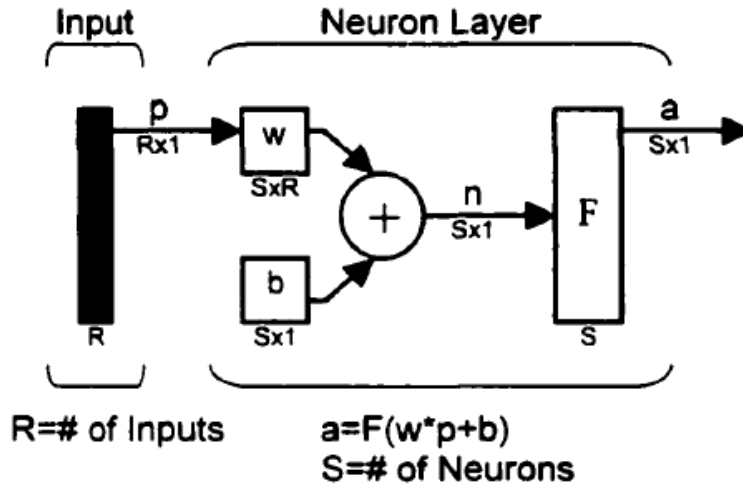
Figure 3- 4 Single-layer Neural Network (Rosenblatt. 1958)

$$w^{SXR} = \begin{bmatrix} w(1.1)w(1.2)...w(1.R) \\ w(2.1)w(2.2)...w(2.R) \\ ...... \\ ...... \\ ...... \\ w(S.1)w(S.2)...w(S.R) \end{bmatrix}$$

(4-3)

In this network, as shown in Figure 4-1 each element of the input vector p is connected to each neuron input through the weight matrix w (Equation 4-3). The *ith* neuron has a summing that gathers its weighted inputs and bias to form its own scalar output $n(i)$. The various $n(i)$ taken together form an S-element vector n. The neuron layer outputs form a colum n vector a. A single-layer network is generally used for simple problem s, while a multiple-layer network can be used to solve complex problems.

3-2-2- 2 Multiple-layer Feedforward Network

A network can have several layers. Each layer has a weight matrix *w,* a bias vector *b.* and an output vector *a.* The network shown below (Figure 4-5) has *R* inputs. SI neurons in the first layer, *S*2 neurons in the second layer, etc. It is common for different layers to have different number of neurons.
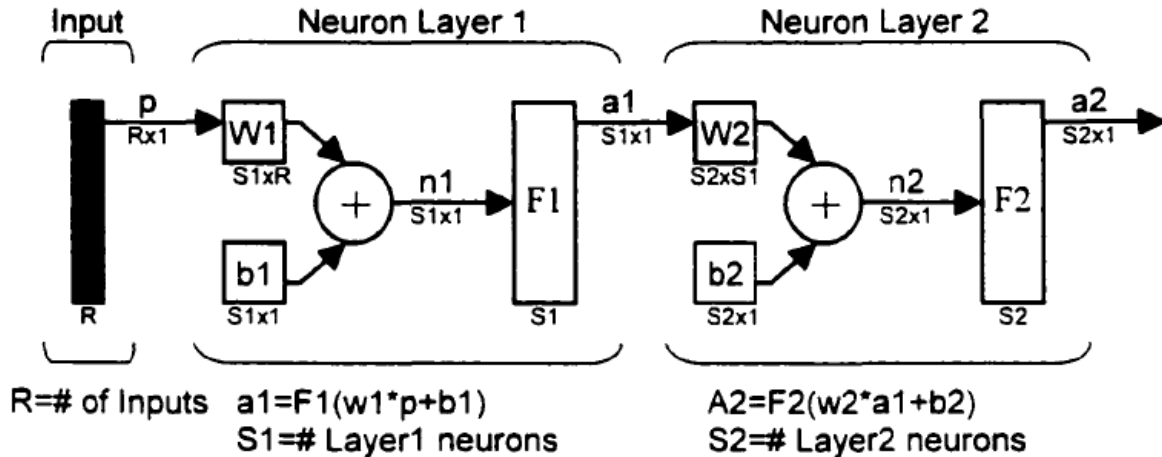
Figure 3- 5 Multiple-Layer Feedforward Network (Rosenbaltt. 1958)

Note that the outputs of the intermediate layer are the inputs to the following layer. Thus, layer 2 can be analyzed as a single layer network with *R - S*1 inputs.

S = *S*2 neurons, and S1x S2 weight matrix w = w2. The input to layer2 is *p* = *a*1. the output is *a* = *a* 2 . Now that all the vectors and matrices of layer2 are identified, it can then be treated as a single layer network on its own. This approach can be taken with any layer of the network.

The layers of a multiple-layer network play different roles. A layer that produces the network output is called an output layer. All other layers are called hidden layers. The two layer networks shown above have one output layer and one hidden layer. Multiple-layer networks are much more powerful than single layer networks since multiple-layer networks are able to use the combination of sigmoid and/or linear transfer functions. Flood (1991) stated that there are many solution surfaces

that are extremely difficult to model using a sigmoidal network using one hidden layer.

In addition, some researchers (Flood and Kartam 1994; Ripley 1996; Sarle 1994) stated that the use of more than one hidden layer provides the flexibility needed to model complex functions in many situations. Lapedes and Farber (1988) provided more practical proof that two hidden layers are sufficient, and according to Chester (1990), the first hidden layer is used to extract the local features of the input patterns while the second hidden layer is useful to extract the global features of the training patterns. However, Masters (1993) stated that using more than one hidden layer often slows the training process dramatically and increases the chance of getting trapped in local minima.

3- 3 Model Optimization (Training)

The process of optimizing the connection weights is known as "training" or "learning". The method most commonly used for finding the optimum weight combination of feed-forward MLP neural networks is the back-propagation algorithm (Rumelhart et al. 1986)

The back-propagation algorithm is a non-linear extension of the least mean squares (LMS) algorithm for multi-layer perceptrons (Brown and Harris 1994). It is the most widely used of the neural network paradigms and has been successfully applied in many fields of model-free function estimation. The back-propagation algorithm generated criticism concerning its ability to converge. The back propagation network (BPN) is expensive computationally, especially during the training process. Many researchers have attempted, therefore, to modify the basic back-propagation algorithm in order to render it suitable to speed training. Properly

trained BPN tends to produce reasonable results when presented with new data set inputs.

3- 4 Stopping Criteria

Stopping criteria are used to decide when to stop the training process. They determine whether the model has been optimally or sub-optimally trained (Maier and Dandy 2000). Many approaches can be used to determine when to stop training. Training can be stopped: after the presentation of a fixed number of training records; when the training error reaches a sufficiently small value; or when no or slight changes in the training error occur. However, the above examples of stopping criteria may lead to the model stopping prematurely or over-training. The *cross-validation* technique (Stone 1974) is an approach that can be used to overcome such problems. It is considered to be the most valuable tool to ensure overfitting does not occur (Smith 1993). Amari et al. (1997) suggested that there are clear benefits in using cross-validation when limited data are available, as is the case for many real-life case studies. The cross-validation technique requires that the data be divided into three sets; training, testing and validation. The training set is used to adjust the connection weights. The testing set measures the ability of the model to generalize, and the performance of the model using this set is checked at many stages of the training process. Training is stopped when the error of the testing set starts to increase. The testing set is also used to determine the optimum number of hidden layer nodes and the optimum values of the internal parameters (learning rate, momentum term and initial weights). The validation set is used to assess model performance once training has been accomplished. A number of different stopping criteria (e.g. Bayesian Information Criterion, Akaike‟s Information Criterion and Final Prediction Error) can also be used, as mentioned

previously. Unlike cross-validation, these stopping criteria require the data be divided into only two sets; a training set, to construct the model; and an independent validation set, to test the validity of the model in the deployed environment. The basic notion of these stopping criteria is that model performance should balance model complexity with the amount of training data and model error.

3- 5 Model Validation

Once the training phase of the model has been successfully accomplished, the performance of the trained model should be validated. The purpose of the model validation phase is to ensure that the model has the ability to generalize within the limits set by the training data in a robust fashion, rather than simply having memorized the input-output relationships that are contained in the training data. The approach is to test the performance of trained ANNs on an independent validation set, which has not been used as part of the model building process. If such performance is adequate, the model is deemed to be able to generalize and is considered to be robust.

The coefficient of correlation, r, the root mean squared error, RMSE, and the mean absolute error, MAE, are the main criteria that are often used to evaluate the prediction performance of ANN models. The coefficient of correlation is a measure that is used to determine the relative correlation and the goodness-of-fit between the predicted and observed data. Smith (1986) suggested the following guide for values of $|r|$ between 0.0 and 1.0:

$|r| \geq 0.8$ strong correlation exists between two sets of variables;

$0.2 < |r| < 0.8$ correlation exists between the two sets of variables; and

$|r| \leq 0.2$ weak correlation exists between the two sets of variables.

The RMSE is the most popular measure of error and has the advantage that large errors receive much greater attention than small errors (Hecht-Nielsen 1990). In contrast with RMSE, MAE eliminates the emphasis given to large errors. Both RMSE and MAE are desirable when the evaluated output data are smooth or continuous (Twomey and Smith 1997).

Investigation into the robustness of ANNs carried out by Shahin et al. (2005c) for a case study of predicting the settlement of shallow foundations on granular soils. found that good performance of ANN models on the data used for model calibration and validation does not guarantee that the models will perform well in a robust fashion over a range of data similar to those used in the model calibration phase. For this reason, Shahin et al. (2005c) proposed a method to test the robustness of the predictive ability of ANN models by carrying out a sensitivity analysis to investigate the response of ANN model outputs to changes in its inputs. The robustness of the model can be determined by examining how well model predictions are in agreement with the known underlying physical processes of the problem in hand over a range of inputs. In addition, Shahin et al. (2005c) also advised that the connection weights be examined as part of the interpretation of ANN model behavior, as suggested by Garson (1991).

They concluded that this approach provided the best overall methodology for quantifying ANN input importance in comparison to other commonly used methods, though with a few limitations.

3-6 Application on Artificial Neural Network in Geotechnical Engineering

Over the last few years or so, the use of artificial neural networks (ANNs) has increased in many areas of engineering. In particular, ANNs have been applied to many geotechnical engineering problems and have demonstrated some degree of

success. A review of the literature reveals that ANNs have been applied successfully to many geotechnical engineering topics such as triaxial compression behavior of sand and gravel (Dayakar et al., 1999), stress- strain modeling of soils (Ellis et al.,1995), capacity of driven piles in cohesionless soils (Abu Kiefa., 1998), assessment of geotechnical properties (Yang and Rosenbaum., 2002), digital soil mapping (Behrens et al., 2005), stability analysis of slopes (Sakellariou and Ferentinou, 2005), and maximum dry density and optimum moisture content prediction of chemical stabilized soil (Alavi et al., 2010).

For brevity, some works are selected to be described in some detail:

3-6- 1 Pile Capacity

Goh (1994a; 1995b) presented a neural network to predict the friction capacity of piles in clays. The neural network was trained with field data of actual case records. The model inputs were considered to be the pile length, the pile diameter, the mean effective stress and the undrained shear strength. The skin friction resistance was the only model output. The results obtained by utilising the neural network were compared with the results obtained by the method of Semple and Rigden (1986) and the â method (Burland 1973). The methods were compared using regression analysis as well as the error rate as shown in Table 3-1. It is evident from Table 1 that ANNs outperform the conventional methods.

Table 3- 1 Summary of correlation coefficients and error rate for friction pile capacity (Goh 1995)

Method	Coefficient of correlation		Error rate (kPa)	
	Training	Testing	Training	Testing
Neural network	0.985	0.956	1.016	1.194
Semple and Rigden (1986)	0.976	0.885	1.318	1.894
â method	0.731	0.704	4.824	3.096

Goh (1995a; 1996b), soon after, developed another neural network to estimate the ultimate load capacity of driven piles in cohesionless soils. In this study, the data used were derived from the results of actual load tests on timber, precast concrete and steel piles driven into sandy soils. The inputs to the ANN model that were found to be more significant were the hammer weight, the hammer drop, the pile length, the pile weight, the pile cross sectional area, the pile set, the pile modulus of elasticity and the hammer type. The model output was the pile load capacity. When the model was examined with the testing set, it was observed that the neural network successfully modelled the pile load capacity. By examining the connection weights, it was observed that the more important input factors are the pile set, the hammer weight and the hammer type. The study compared the results obtained by the neural networks with the following common relationships: the Engineering News formula (Wellington 1892), the Hiley formula (Hiley 1922) and the Janbu formula (Janbu 1953). Regression analysis was carried out to obtain the coefficients of correlation of predicted versus measured results for neural networks and the traditional methods. Table 3-2 summarises the regression analysis results which indicate that the neural network predictions of the load capacity of driven piles were found to be better than these obtained using the other methods.

Table 3- 2 Summary of regression analysis results of pile capacity prediction (Goh 1995)

Method	Coefficient of correlation	
	Training data	Testing data
Neural network	0.96	0.97
Engineering News	0.69	0.61
Hiley	0.48	0.76
Janbu	0.82	0.89

Lee and Lee (1996) utilised neural networks to predict the ultimate bearing capacity of piles. The problem was simulated using data obtained from model pile load tests using a calibration chamber and results of in-situ pile load tests. For the simulation using the model pile load test data, the model inputs were the penetration depth ratio (i.e. penetration depth of pile/pile diameter), the mean normal stress of the calibration chamber and the number of blows.

The ultimate bearing capacity was the model output. The prediction of the ANN model showed maximum error not more than 20% and average summed square error less than 15%. For the simulation using the in-situ pile load test data, five input variables were used representing the penetration depth ratio, the average standard penetration number along the pile shaft, the average standard penetration number near the pile tip, pile set and hammer energy. Two neural network models were developed. The results of these models were compared with Meyerhof's equation (Meyerhof 1976) based on the average standard penetration value. Figure 4 shows the plots of the testing set results of estimated versus measured pile bearing capacity obtained from the neural network models and Meyerhof's equation. The plots in Figure 3-6 show that the predicted values from the neural networks matched the measured values much better than those obtained from Meyerhof's equation.
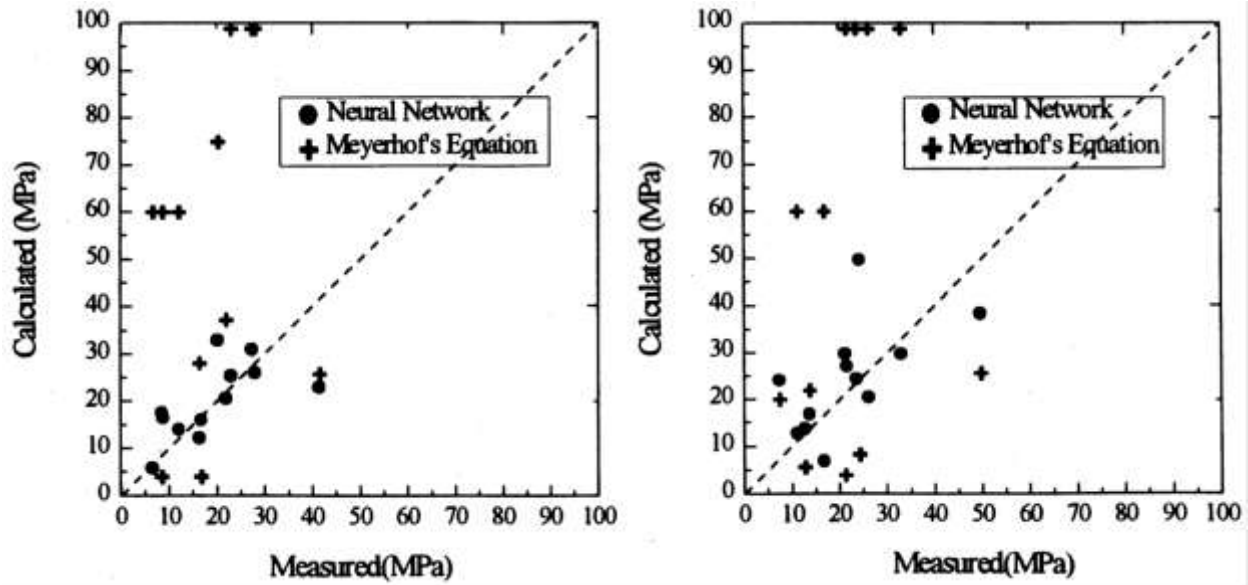
Figure 3- 6 Testing results of predicted vs measured pile bearing capacity from in-situ pile load test
(Lee and Lee 1996)

Abu-Kiefa (1998) introduced three neural networks to predict the capacity of driven piles in cohesionless soils. The first model was developed to estimate the total pile capacity. The second model was employed to estimate the tip pile capacity, whereas the final model was used to estimate the shaft pile capacity. Five variables were selected to be the model inputs in the first and second model. These inputs were the angle of shear resistance of the soil around the shaft, the angle of shear resistance at the tip of the pile, the effective overburden pressure at the tip of the pile, the pile length and the equivalent cross-sectional pile area. The model had one output representing the total pile capacity. The input variables used to predict the pile shaft capacity were four, representing the average standard penetration number around the shaft, the angle of shear resistance around the shaft, pile length and pile diameter. The results of the networks obtained in this study were compared with four other empirical techniques.

These techniques were those proposed by Meyerhof (1976), Coyle and Castello (1981), the American Petroleum Institute (1984) and Randolph (1985). The results of the total pile capacity prediction demonstrated high coefficients of

determination (0.95) for all data records obtained from the neural network model, while they ranged between 0.52 and 0.63 for the other methods. Figures 3-7 to 3-9 show the measured versus predicted values of all data records for the pile capacity, tip pile capacity and shaft pile capacity, respectively. It can be seen from these figures that the predictions of the neural networks produce less scatter than the predictions of all other methods, and thus provide the best prediction of pile load capacity, tip pile capacity and shaft pile capacity.
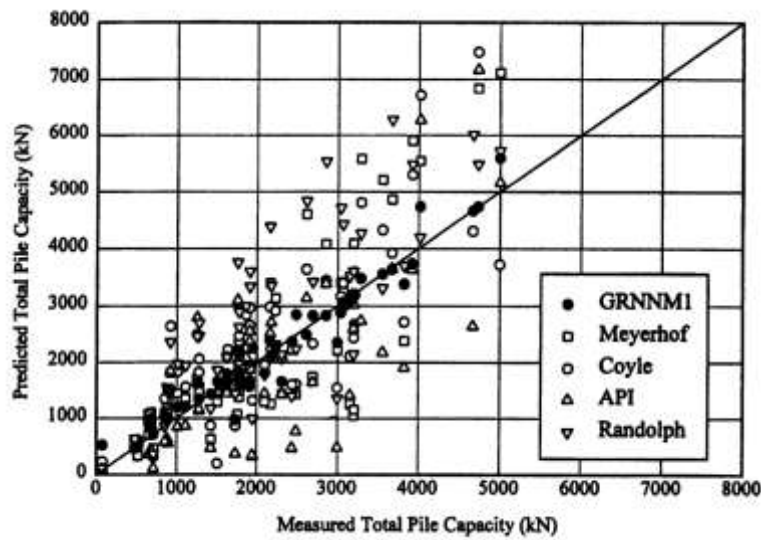
Figure 3- 7 Comparison of predicted and measured total pile capacity (Abu-Kiefa 1998)
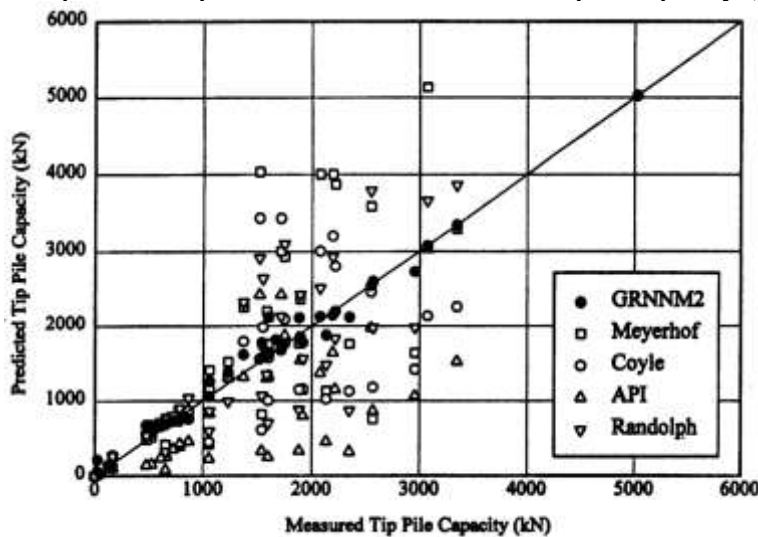
Figure 3- 8 Comparison of predicted and measured tip pile capacity (Abu-Kiefa 1998)
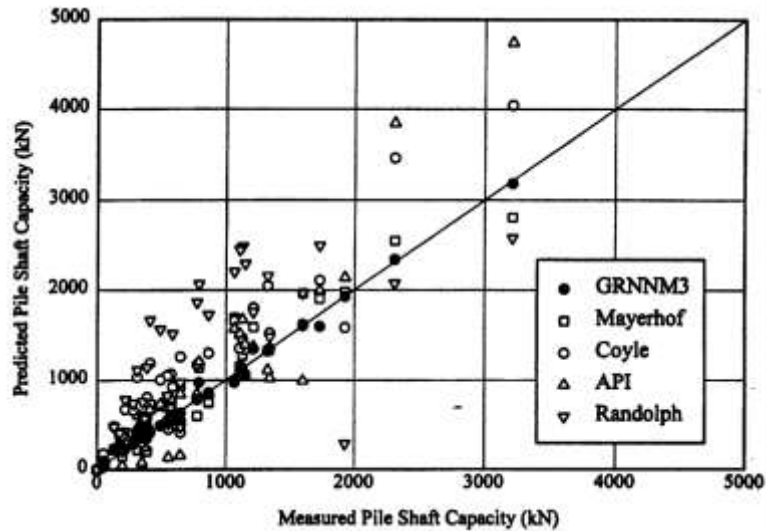
Figure 3- 9 Comparison of predicted and measured shaft pile capacity (Abu-Kiefa 1998)

3-6- 2 Settlement of Foundation

The design of foundations is generally controlled by the criteria of bearing capacity and settlement; the latter often governing. The problem of estimating the settlement of foundations is very complex, uncertain and not yet entirely understood. This fact encouraged some researchers to apply the ANN technique to settlement prediction. Goh (1994a) developed a neural network for the prediction of settlement of a vertically loaded pile foundation in a homogeneous soil stratum. The input variables for the proposed neural network consisted of the ratio of the elastic modulus of the pile to the shear modulus of the soil, pile length, pile load, shear modulus of the soil, Poisson's ratio of the soil and radius of the pile. The output variable was the pile settlement. The desired output that was used for the ANN model training was obtained by means of finite element and integral equation analyses developed by Randolph and Wroth (1978). A comparison of the theoretical and predicted settlements for the training and testing sets is given in Figure 3-10. The results in Figure 3-10 show that the neural network was able to successfully model the settlement of pile foundations.
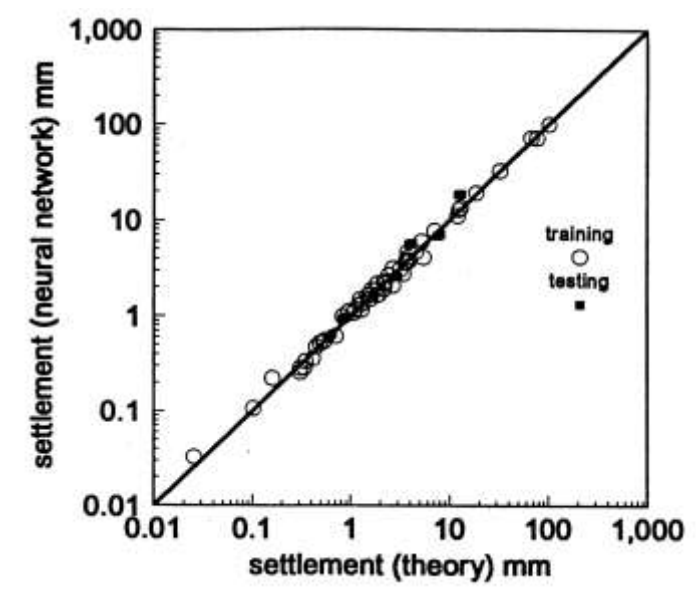
Figure 3- 10 Comparison of theoretical settlements and neural network predictions (Goh 1994)

Most recently, Shahin et al. (2000) carried out similar work for predicting the settlement of shallow foundations on cohesionless soils. In this work, 272 data records were used for modelling. The input variables considered to have the most significant impact on settlement prediction were the footing width, the footing length, the applied pressure of the footing and the soil compressibility. The results of the ANN were compared with three of the most commonly used traditional methods. These methods were Meyerhof (1965), Schultze and Sherif (1973) and Schmertmann et al. (1978).

The results of the study confirmed those found by Sivakugan et al. (1998), in the sense that ANNs were able to predict the settlement well and outperform the traditional methods. As shown in table 3-3, the ANN produced high coefficients of correlation, r, low root mean squared errors, RMSE, and low mean absolute errors, MAE, compared with the other methods.

Table 3- 3 Comparison of predicted vs measured settlements (Shahin et al. 2000)

Category	ANN	Meyerhof (1965)	Schultze & Sherif (1973)	Schmertmann et al. (1978)
Correlation, r	0.99	0.33	0.86	0.70
RMSE (mm)	3.9	27.0	23.8	45.2
MAE (mm)	2.6	20.8	11.1	29.5

3-6- 3 Liquifaction

Liquefaction is a phenomenon which occurs mainly in loose and saturated sands as a result of earthquakes. It causes the soil to lose its shear strength due to an increase in pore water pressure, often resulting in large amounts of damage to most civil engineering structures. Determination of liquefaction potential due to earthquakes is a complex geotechnical engineering problem. Goh (1994b) used neural networks to model the complex relationship between seismic and soil parameters in order to investigate liquefaction potential. The neural network used in this work was trained using case records from 13 earthquakes that occurred in Japan, United States and Pan-America during the period 1891–1980. The study used eight input variables and only one output variable. The input variables were the SPT-value, the fines content, the mean grain size, the total stress, the effective stress, the equivalent dynamic shear stress, the earthquake magnitude and the maximum horizontal acceleration at ground surface. The output was assigned a binary value of 1, for sites with extensive or moderate liquefaction, and a value of 0 for marginal or no liquefaction. The results obtained by the neural network model were compared with the method of Seed et al. (1985). The study showed that the neural network gave correct predictions in 95% of cases, whereas Seed et

al. (1985) gave a success rate of 84%. Goh (1996a) also used neural networks to assess liquefaction potential from cone penetration test (CPT) resistance data. The data records were taken for sites of sand and silty sand deposits in Japan, China, United States and Romania, representing five earthquakes that occurred during the period 1964–1983. A similar neural network modelling strategy, as used in

Goh (1994b), was used for this study and the results were compared with the method of Shibata and Teparaksa (1988).

The neural network showed a 94% success rate, which is equivalent to the same number of error predictions as the conventional method by Shibata and Teparaksa (1988).

Two other works (Najjar and Ali 1998; Ural and Saka 1998) also used CPT data to evaluate soil liquefaction potential and resistance. Najjar and Ali (1998) used neural networks to characterise the soil liquefaction resistance utilising field data sets representing various earthquake sites from around the world. The ANN model that was developed in this work was generated to produce a liquefaction potential assessment chart that could be used by geotechnical engineers in liquefaction assessment tasks. Ural and Saka (1998) used neural networks to analyse liquefaction. Comparison between this approach and a simplified liquefaction procedure indicated a similar rate of success for the neural network approach as the conventional approach.

Other applications of ANNs for liquefaction prediction include the prediction of liquefaction resistance and potential (Juang and Chen 1999), investigation of the accuracy of liquefaction prediction of ANNs compared with fuzzy logic and statistical approaches (Ali and Najjar 1998) and assessment of liquefaction potential using standard penetration test results (Agrawal et al. 1997).

3-6- 4 Slope Stability

Ni et al. (1996) proposed a methodology of combining fuzzy sets theory with artificial neural networks for evaluating the stability of slopes. In this approach, the input parameters were gradient, horizontal profile, vertical profile, location, height, geological origin, soil texture, depth of weathering, direction of slopes, vegetation, land use, maximum daily precipitation and maximum hour precipitation. The output was the slope failure potential. A number of hypothetical natural slopes were evaluated by both neural networks and an analytical model, and the results of the neural network approach were in a good agreement when compared with those obtained by the analytical model.

CHAPTER 4
STABILITY EVALUATION OF PO RIVER BANKS

4- 1 Introduction

In the assessment of slopes, engineers primarily use FS values to determine how close or far slopes are from failure. Conventional limit-equilibrium techniques are the most commonly-used analysis methods (Haut., 2006; Mwasha., 2008; Ozcep., 2010; Sharma., 2011). Recently, elasto-plastic analysis of geotechnical problems using finite element (FE) method has been widely accepted in the research arena for many years. Slope stability represents an area of geotechnical analysis in which a nonlinear finite element approach offers real benefits over existing methods. Slope stability analysis by elasto-plastic FE is accurate, robust and simple enough for routine use by practicing engineers.

 The main advantages of the FE approach over traditional limit equilibrium methods for slope stability analysis are that no assumption needs to be made in advance about the shape or location of the failure surface, slice side forces and their directions and the slip surface could be of any shape (Chollada, 2013). General soil material models that include Mohr-Coulomb and numerous others can be employed.

Limit equilibrium methods only give an estimate of FS with no information on deformation of the slope. In numerical analysis, failure occurs "Naturally" which evolve during the calculation in a way that is representative of the natural evolution of the physical failure plane in the slope (Wyllie and Mah, 2004).

The FE code Plaxis2D version 2012 in conjunction with an elastic-perfectly plastic (Mohr-Coulomb) stress strain model has been used for the stability analysis of river banks along the Po River the main in Italy, under various river and

groundwater boundary conditions in this study. The Mohr-Coulomb failure criterion is currently the most widely used method for soil in practical applications (El-Naggar, 2010). The Mohr–Coulomb model is a linearly elastic and perfectly plastic constitutive model. The parameters needed for the Mohr–Coulomb model are the Young's modulus (E) and Poisson's ratio (ν) for the elastic strain component of the soil behavior. The effective strength parameters cohesion (c'), and friction angle (φ'), as well as the dilatancy angle (ψ) are needed for the plastic strain component of the soil behavior.

4- 2 Study Area

The Po River is known as the longest river entirely flowing in the Italian peninsula. The main stream of this river is about 652 km long. It is also the Italian river with the most extended catchment, stretches across northern Italy from the French border on the west to the Adriatic Sea on the east whose area is about 71000 km2 at the delta. Figure 4-1 presents a schematic map of the Po River basin. The river is subject to heavy flooding. Consequently more than half its total length is immured by man-maded fine-grained earthen embankments called *argini.*

In order to gain a better understanding of the behaviors of the river regime, the hydrological behaviors of the Po River have been extensively studied, especially for what refers to the flood regime (Marchi, 1994; Visentini, 1953; Piccoli, 1976; Zanchettini et al., 2008; Montanari., 2012). The average yearly water flow at the estuary is 1460 m^3. The Po River has the Alpine water regime on its higher course. During which the water level of the river Po and its tributaries rises by 5 to 10 meters. The history of the Po River floods is well known. In fact, starting from the middle age the lands surrounding the river were intensively cultivated and since that time they were recorded. By observing their frequency, one may assess that

events with about 5-year return period were recorded. Since the area is characterized by a very high concentration of population and industrial activities, evaluation of embankment along the Po River is crucial. This study investigates the Po river banks slope stability using the ANN method.

The engineering properties of body of the embankments and the foundation soils were investigated by in situ tests. Results from the experimental activities and their interpretation were applied to generate minimum FS of 77 river banks with different geometry and shear strength parameters using the FE method in conjunction with an elastic-perfectly plastic (Mohr-Coulomb) stress strain model. Each section of the Po river bank is evaluated under two different water level according to low level of water in river and high water stage in Po.

Figure 4- 1 Map of the Po River basin (from Wikipedia)

4- 3 Plaxis2D

Plaxis is an FE computer programming which is mainly used for the stress-deformation analysis; stability and leakage analysis in geotechnical projects.

In general, the analysis in Plaxis includes:

1. Defining the geometry and FE model layout

2. Specifying material parameters: appropriate selection of material strength and stiffness parameters from laboratory or in-situ tests.

3. Generating stresses.

4. Construction staging i.e. defining various stages of excavation using staged construction.

After defining the geometry of the problem, assigning geotechnical specifications of soil layers and water table and stress-strain and safety analysis are done through four phases by stage construction capability of the software (Plaxis 2D 2011).

- **Determination of the Factor of Safety**

The FS of a soil slope is defined here as the factor by which the original shear strength parameters must be divided in order to bring the slope to the point of failure. The factored shear strength parameters (c'_f and $\emptyset'_f$) are therefore given *by:*

$$c'_f = {c'}/{SRF} \tag{4-1}$$

$$\emptyset'_F = arctan\left(\frac{\tan \emptyset'}{SRF}\right) \tag{4-2}$$

where SRF is a "Strength Reduction Factor". This method is referred to as the "shear strength reduction technique" (e.g. Matsui and San 1992; Griffi and Lane, 1999) and allows for the interesting option of applying different strength reduction factors to the c' and ´ terms. In this paper, however, the same factor is always applied to both terms. To find the true FS, it is necessary to initiate a systematic search for the value of SRF that will cause the slope to fail. When this value has been found, FS = SRF

4- 4 Data Availability and Slope Stability

4-4- 1Soil Stratigraphy with the Use of Cone penetration testing with pore-water pressure measurement (CPTu)

The electric Cone Penetration Test (CPT) has been in use for over 40 years. The CPT has major advantages over traditional methods of field site investigation such as drilling and sampling since it is fast, repeatable and economical. In addition, it provides near continuous data and has a strong theoretical background. These advantages have led to a steady increase in the use and application of the CPT in many places around the world.

In order to obtain the soil stratigraphy, physical and mechanical properties of subsurface strata and groundwater conditions, 220 cone penetration tests have been conducted on 77 embankments along the Po river.

Numerous correlations have been developed to estimate geotechnical parameters from the CPTu for a wide range of soils. These correlations vary in their reliability and applicability.

Based on most reliable and recent empirical and semi empirical correlations a program is set up. Following, equations 4-3 to 4-26, is the body of equations that have been used in this investigation to interpret the CPTu results in order to find out the soil classification (Robertson, 2010; Robertson and Cabal, 2011). A schematic view of the developed program in excell is shown in tablaes 4-1 and 4-2. Table 4-1 contains the input values driven direcly from the CPTu test and the soil index parameters as outputs of the program are shown in table 4-2

CPTu Interpretation- Body of Equations

[1] Cone resistance [MPa]:

$$q_c = \frac{Q_c}{A_c} \tag{4-3}$$

Q_c: The force acting on the cone

A_c: Area of the cone

[2] Corrected cone resistance [MPa]:

$$q_t = q_c + u_2(1 - a) \tag{4-4}$$

$a = 0.7 - 0.85$ (Depends on the device)

u_2: Measured pore pressere

For sandy soils, a=1

[3] Net cone resistance [MPa]:

$$q_n = q_t - \sigma_{v0} \tag{4-5}$$

$\sigma_{v0} = In - situ$ total stress

[4] Normalized cone resistance:

$$Q_t = \frac{q_t - \sigma_{v0}}{\sigma'_{v0}} \tag{4-6}$$

$\sigma'_{v0} = In - situ$ vertical effective stress

[5] Normalized cone resistance:

$$Q_{tn} = \left[\frac{q_t - \sigma_{v0}}{p_{a2}}\right] \left[\frac{p_a}{\sigma'_{v0}}\right]^n \tag{4-7}$$

n: Depends on soil type and stress levl

p_a: Atmospheric pressure

[6] Pore pressure ratio:

$$B_q = \frac{\Delta u}{q_n} \tag{4-8}$$

$$\Delta u = u_2 - u_0 \tag{4-9}$$

$u_0: In-situ\ equilibrium\ pore\ pressure$

[7] Sleeve friction [MPa]:

$$f_s = \frac{F_s}{A_s} \tag{4-10}$$

F_s = The frriction force acting on fricion sleeve

A_S: The area of the friction sleeve

[8] Friction ratio:

$$R_f = \frac{f_s}{q_t} \times 100\% \tag{4-11}$$

[9] Soil Behavior Type Index:

$$I_c = ((3.47 - \log Q_t)^2 + (\log F_r + 1.22)^2)^{0.5} \tag{4-12}$$

[10] Unit eight of soil [MN/m3] (Robertson2010):

$$\gamma = \gamma_w 0.27 \log \left(R_f + 0.36 \log \frac{q_t}{p_a} + 1.236 \right) \tag{4-13}$$

γ_w: Unit weight of water

[11] Drained Young's modulus [MPa](Robertson 2009):

$$E = (q_t - \sigma_v) \times 0.015 \times 10^{0.55 I_c + 1.68} \tag{4-14}$$

Note: For silica sands

[12] Small strain shear modulus [MPa] (Eslaamizaad&Robertson 1996):

$$G_0 = (q_t - \sigma_v) \times 0.0188 \times 10^{0.55 I_c + 1.68} \tag{4-15}$$

Note: For Wide range of Soils

[13] Equivalent SPT N60 (Jefferies&Davies 1993):

$$N_{SPT} = N_{60} = \frac{q_c}{p_a} \times \frac{1}{10^{1.1268-0.2827I_c}} \tag{4-16}$$

Note: Does not work good in stiff clays

[14] Peak drained friction angle (Kulhawy & Mayne 1990):

$$\emptyset' = 17.6 + 11 \times \log Q_t \tag{4-17}$$

SBT= 5,6,7,8

[15] Effective stress friction angle (Mayne 2005):

$$\emptyset' = 29.5 \times B_q^{0.121} \tag{4-18}$$

$0.1 < B_q < 1$

$20 < \emptyset' < 45$

Note: Apply to normally to lightly over consolidated clays- For small and medium projects- For heavily over consolidated clays the lab tests should be done.

[16] In situ stress ratio (Kulhawy&Mayne 1990):

$$K_0 = 0.1 \frac{q_t - \sigma_v}{\sigma_v'} = 0.1 Q_t \tag{4-19}$$

$0.1 < B_q < 1$

[17] Untrained peak shear strength [kPa] (All theories):

$$S_u = \frac{(q_t - \sigma_v)}{N_{kt}} = \frac{q_n}{N_{kt}} \tag{4-20}$$

$$N_{kt} = 10.50 + 7 \log(F_r) \tag{4-21}$$

SBT= 1,2,3,4,9

[18] Remolded undrained shear strength [kPa]:

$$S_{u(Remolded)} = f_s \tag{4-22}$$

SBT=1,2,3,4,9

[19] Soil sensitivity:

$$S_t = \frac{S_u}{S_{u(Remolded)}}$$

(4-23)

[20] Shear wave velocity [m/s]:

$$V_s = \frac{G_0}{\rho}$$

(4-24)

[21] Permeability [m/s] (Robertson 2010):

$$K = 10^{0.952 - 3.04 \times I_c} \qquad 1 < I_c < 3.27$$

(4-25)

$$K = 10^{-4.52 - 1.37 \times I_c} \qquad 3.27 < I_c < 4$$

(4-26)

Table 4- 1 Developed program for interpreting the CPTu tests- Inputs

Profondità Misurata [m]	Profondità Corretta [m]	Deviazione dalla verticale [m]	Profondità Friction [m]	q_t [MPa]	f_s [MPa]	u [MPa]	Risultante inclinometri [Gradi]	U_0 [Mpa]
0.025	0.025	0.000	-0.045	0.43786	0.00349	0.00012	0.44	0
0.033	0.033	0.000	-0.037	0.45475	0.00326	0.00070	0.43	0
0.041	0.041	0.000	-0.029	0.64587	0.00277	0.00012	0.40	0
0.050	0.050	0.000	-0.020	0.77348	0.00279	0.00070	0.33	0
0.058	0.058	0.000	-0.012	0.80368	0.00307	0.00070	0.53	0
0.066	0.066	0.000	-0.004	0.98125	0.00310	-0.00046	0.32	0
0.074	0.074	0.001	0.004	1.01156	0.00297	0.00012	0.53	0
0.082	0.082	0.001	0.012	1.04511	0.00318	0.00012	0.30	0
0.091	0.091	0.001	0.021	1.15907	0.00395	-0.00046	0.54	0
0.099	0.099	0.001	0.029	1.12910	0.00408	0.00070	0.44	0
0.107	0.107	0.001	0.037	1.10539	0.00430	-0.00046	0.46	0
0.115	0.115	0.001	0.045	1.25960	0.00410	-0.00104	0.25	0
0.123	0.123	0.001	0.053	1.22640	0.00430	0.00070	0.55	0
0.131	0.131	0.001	0.061	1.27325	0.00455	0.00012	0.37	0
0.139	0.139	0.001	0.069	1.36025	0.00489	-0.00104	0.55	0

Table 4-1 Continue

q_c [MPa]	F_R %	γ [kN/m³]	σ_{v0} [MPa]	σ'_{v0} [MPa]	q_n [MPa]	B_q	Q_t	R_f Normalized %
0.4378399	0.7970932	14.38	0.0003596	0.0003593	0.43744	N/A	2499.7433	0.797867622
0.454615	0.7173918	14.32	0.0004725	0.0004722	0.45419	N/A	1966.2751	0.718277812
0.6458512	0.428659	14.26	0.0005848	0.0005844	0.64518	N/A	2248.0814	0.429122067
0.7733419	0.3604768	14.34	0.0007171	0.0007166	0.77263	N/A	2207.5851	0.360873315
0.8035371	0.3824674	14.47	0.0008393	0.0008387	0.80269	N/A	1977.1335	0.382937166
0.9813434	0.3163635	14.56	0.000961	0.0009603	0.98013	N/A	2121.5555	0.316725601
1.0115385	0.2934145	14.52	0.0010744	0.0010737	1.01030	N/A	1950.4555	0.293779859
1.0450887	0.3041243	14.61	0.0011982	0.0011974	1.04372	N/A	1818.3787	0.304530442
1.1591594	0.3408051	14.91	0.0013566	0.0013557	1.15752	N/A	1817.2	0.341260554
1.1289642	0.3610475	14.94	0.0014785	0.0014775	1.12742	N/A	1626.9201	0.361586444
1.1054791	0.38891	14.99	0.0016038	0.0016027	1.10357	N/A	1473.4343	0.389551008
1.25981	0.3253726	14.98	0.0017231	0.001722	1.25765	N/A	1562.3408	0.325878381
1.2262598	0.350624	15.03	0.0018486	0.0018474	1.22431	N/A	1422.0043	0.351222844
1.2732301	0.3576679	15.11	0.0019796	0.0019783	1.27103	N/A	1386.1123	0.358294597
1.3604606	0.3596332	15.22	0.0021157	0.0021144	1.35789	N/A	1395.6134	0.360259008

Table 4- 2 Developed program for interpreting the CPTu tests- Outputs

I_c	Soil Behavior Type	E´	G_0	K	N_{SPT}	$\phi´$
		[MPa]	[MPa]	m/day		[°]
1.12	Sand Mixtures- Silty Sand to Sandy Silt (5)	15.2	19.0	0.399856	4.4	45.4
1.09	Sand Mixtures- Silty Sand to Sandy Silt (5)	14.9	18.7	0.297402	4.2	45.0
0.86	Sand Mixtures- Silty Sand to Sandy Silt (5)	14.8	18.6	0.329316	4.2	45.0
0.79	Sand Mixtures- Silty Sand to Sandy Silt (5)	14.6	18.3	0.301699	4.1	44.8
0.82	Sand Mixtures- Silty Sand to Sandy Silt (5)	14.4	18.0	0.203901	3.9	44.3
0.73	Sand Mixtures- Silty Sand to Sandy Silt (5)	14.3	17.9	0.199819	3.9	44.2
0.71	Sand Mixtures- Silty Sand to Sandy Silt (5)	14.2	17.8	0.198701	3.9	44.2
0.73	Sand Mixtures- Silty Sand to Sandy Silt (5)	14.2	17.8	0.239397	3.9	44.3
0.78	Sand Mixtures- Silty Sand to Sandy Silt (5)	14.0	17.5	0.173574	3.8	43.8
0.82	Sand Mixtures- Silty Sand to Sandy Silt (5)	14.0	17.6	0.156815	3.8	43.7
0.86	Sand Mixtures- Silty Sand to Sandy Silt (5)	14.2	17.8	0.178793	3.9	43.9
0.78	Sand Mixtures- Silty Sand to Sandy Silt (5)	14.1	17.6	0.117649	3.7	43.4
0.83	Sand Mixtures- Silty Sand to Sandy Silt (5)	14.0	17.6	0.124096	3.7	43.4
0.84	Sand Mixtures- Silty Sand to Sandy Silt (5)	14.0	17.5	0.122030	3.7	43.3
0.84	Sand Mixtures- Silty Sand to Sandy Silt (5)	13.9	17.4	0.148440	3.7	43.4

4-4- 2Slope stability analysis

The FE stability analysis with Plaxis2D and steady state seepage analysis was conducted for each section of Po river embankments for low and high water level in river. In each section the body of the embankment and the soil layer beneath the embankment, two different water levels are considered in the analyses.

The calculation consists of four phases. In the initial phase, initial stresses and initial pore water pressure in low water level condition are calculated using Gravity Loading. For this situation, the water pressure distribution is calculated using a steady-state groundwater flow calculation. This phase is followed by so called 'nil step' to increase the accuracy of the stress field, before considering the high water level situation. The third phase considers the long term behavior of the river bank at high level of river water, which involves a steady-state groundwater flow

calculation to calculate water pressure distribution. Finally for all tow water pressure situations the FS of the bank is calculated by means of phi-c reduction.

In the Plaxis2D analysis, additional displacements are generated during a safety calculation. The total incremental displacement in the final step (at failure) gives an indication of the likely failure mechanism (Figure 2(c) and (d)). The soil layers were modeled using 15-node triangular elements. The powerful 15-node element provides an accurate calculation of stresses and failure nodes. Due to a stress concentration around the toe of embankment, a finer FE mesh is used in these areas and mesh became coarser in the zones away from the toe. As an example of the works that are done on 77 sections of Po river embankments, the geological map with the location of CPTu tests, the results of CPTu tests and the soil stratigraphy driven from the CPTu results for a two selected river banks is shown in figure 4-2(a) to (e) and 4-5(a) to (e). Then the developed FE model, and the failure mechanism in two different water levels for the first section is presented in figure 4-3(a) to (c). As indicated before the sections have been simplified to be investigated with ANN method. The simplified geometry and the FE stability analysis on two selected simplified section in two different water levels is shown in figure 4-4(a) to (c) and 4-6 (a) and (b).

(a) Geological Map of Section U204-205-206FEN

| q_t (MPa) | U (MPa) | fs (MPa) | SBT | θ' |
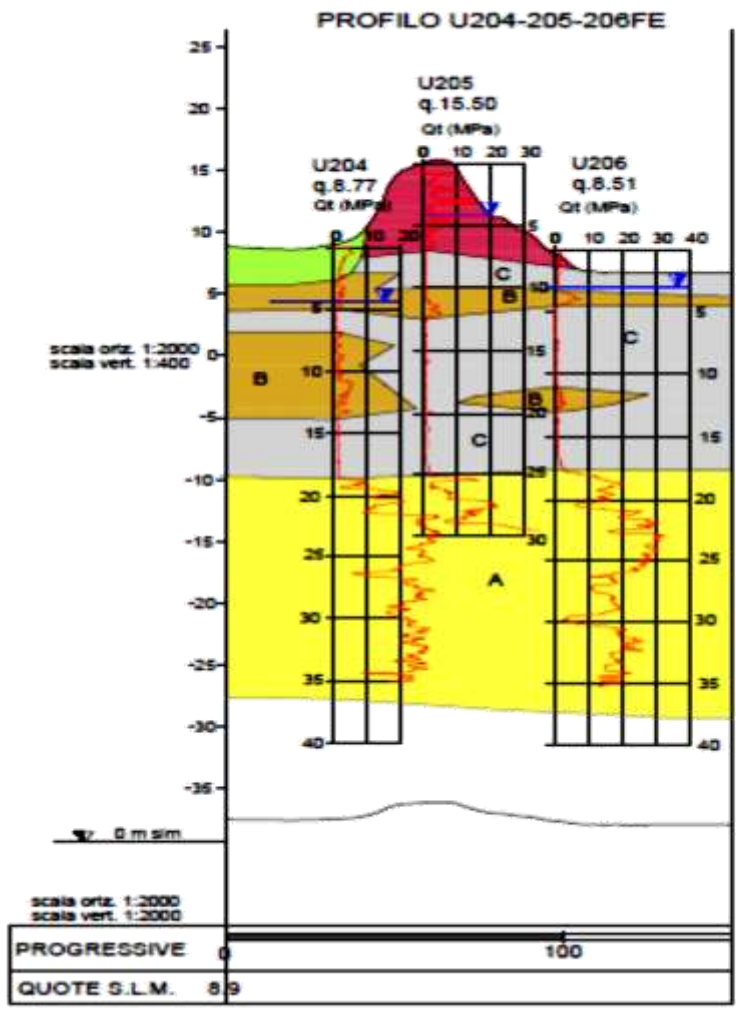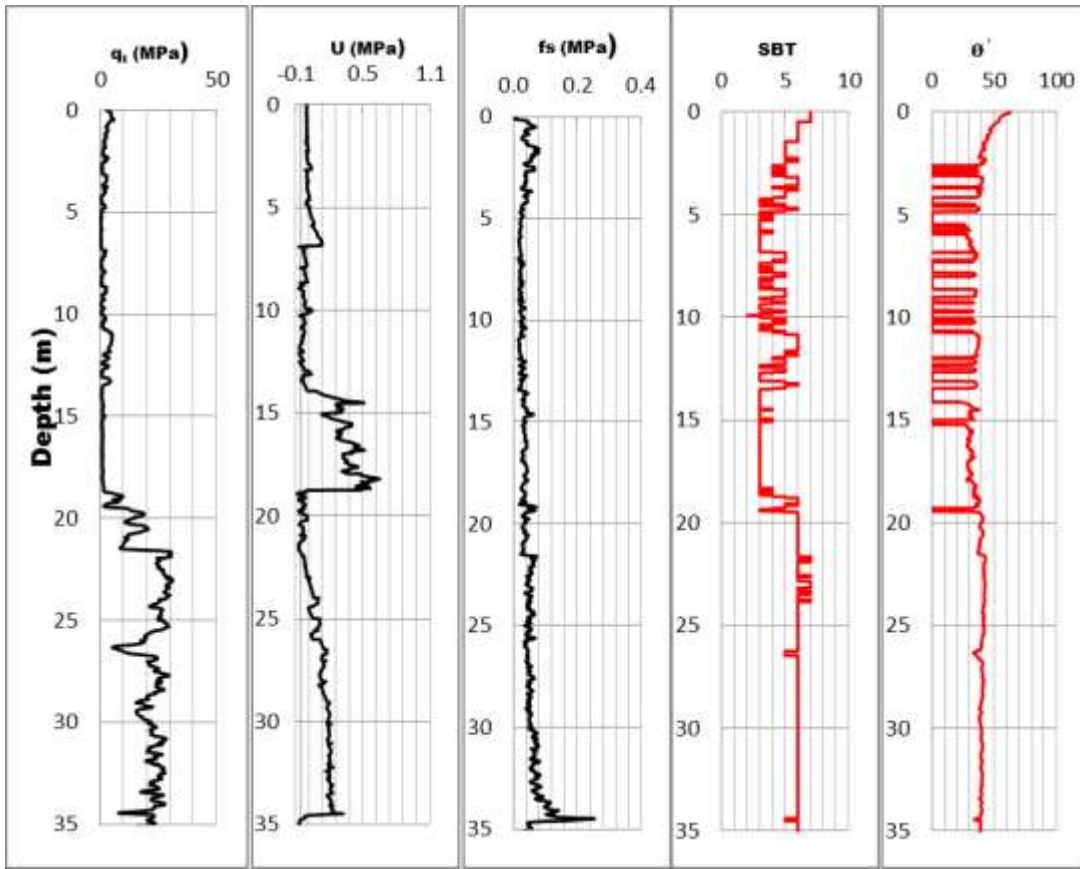
Depth[m]		Ic Average	SBT			
0	2.5	1.89	Alluvial	Es	[MPa]	18
				G0	[MPa]	23
				K	m/s	1E-04
				φ	[°]	44
2.5	5	2.44	Silt mixtures-clayey silt to silty caly	Es	[MPa]	14
				G0	[MPa]	25
				K	m/s	3E-06
				φ	[°]	24
5	7	3.15	Clays- Silty day to clay	Es	[MPa]	0
				G0	[MPa]	19
				K	m/s	5E-09
				φ	[°]	19
7	13.5	2.59	Silt mixtures-clayey silt to silty caly	Es	[MPa]	16
				G0	[MPa]	35
				K	m/s	3E-06
				φ	[°]	18
13.5	18.5	3.17	Clays- Silty day to clay	Es	[MPa]	0
				G0	[MPa]	42
				K	m/s	3E-09
				φ	[°]	26
18.5	35	1.59	Sands- Clean sand to silty sand	Es	[MPa]	107
				G0	[MPa]	135
				K	m/s	3E-04
				φ	[°]	40

(b) Cptu results and soil profile of U204FEN
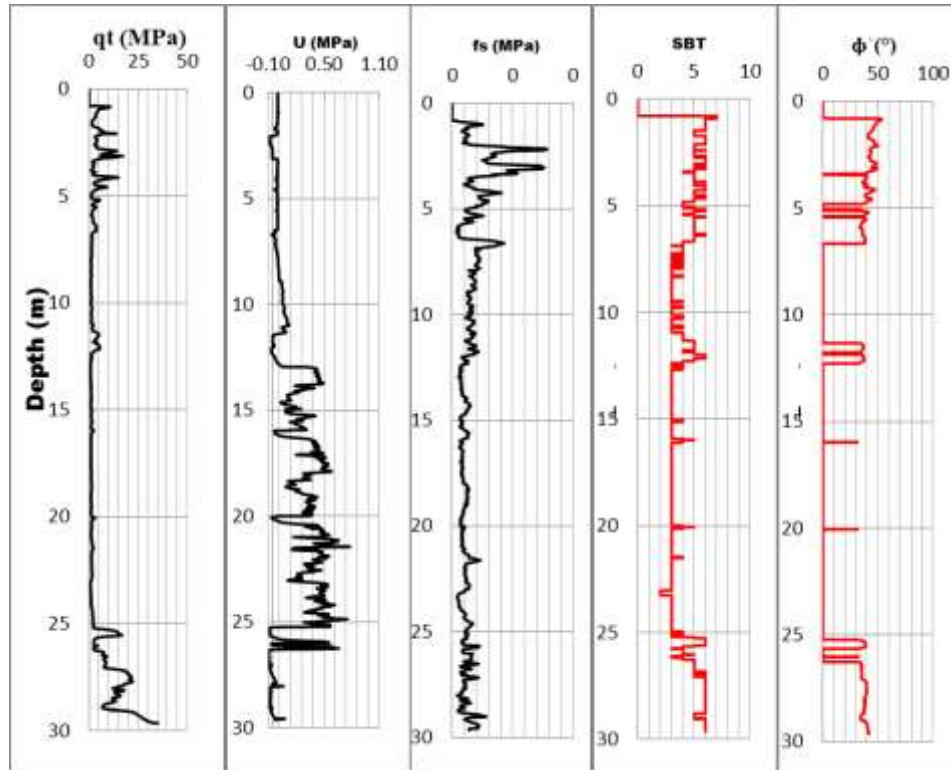
Depth(m)		Ic Average	SBT			
+6.432	-1.068	2.19	Sand mixtures silty sand to sandy silt	Es	[MPa]	30
				G0	[MPa]	45
				K	m/s	5E-05
				φ	[°]	34
				Su	[kPa]	0
-1.068	-4.568	3.01	Clays- Silty clay to clay	Es	[MPa]	0
				G0	[MPa]	44
				K	m/s	7E-09
				φ	[°]	0
				Su	[kPa]	0
-4.568	-6.068	2.54	Sand mixtures silty sand to sandy silt	Es	[MPa]	25
				G0	[MPa]	55
				K	m/s	1E-06
				φ	[°]	18
				Su	[kPa]	0
-6.068	-18.568	3.20	Clays- Silty clay to clay	Es	[MPa]	0
				G0	[MPa]	49
				K	m/s	4E-09
				φ	[°]	0
				Su	[kPa]	0
-18.568	-28.568	1.96	Sands- clean sand to silty sand	Es	[MPa]	82
				G0	[MPa]	114
				K	m/s	8E-05
				φ	[°]	32
				Su	[kPa]	0

(c) Cptu results and soil profile of U205FEN
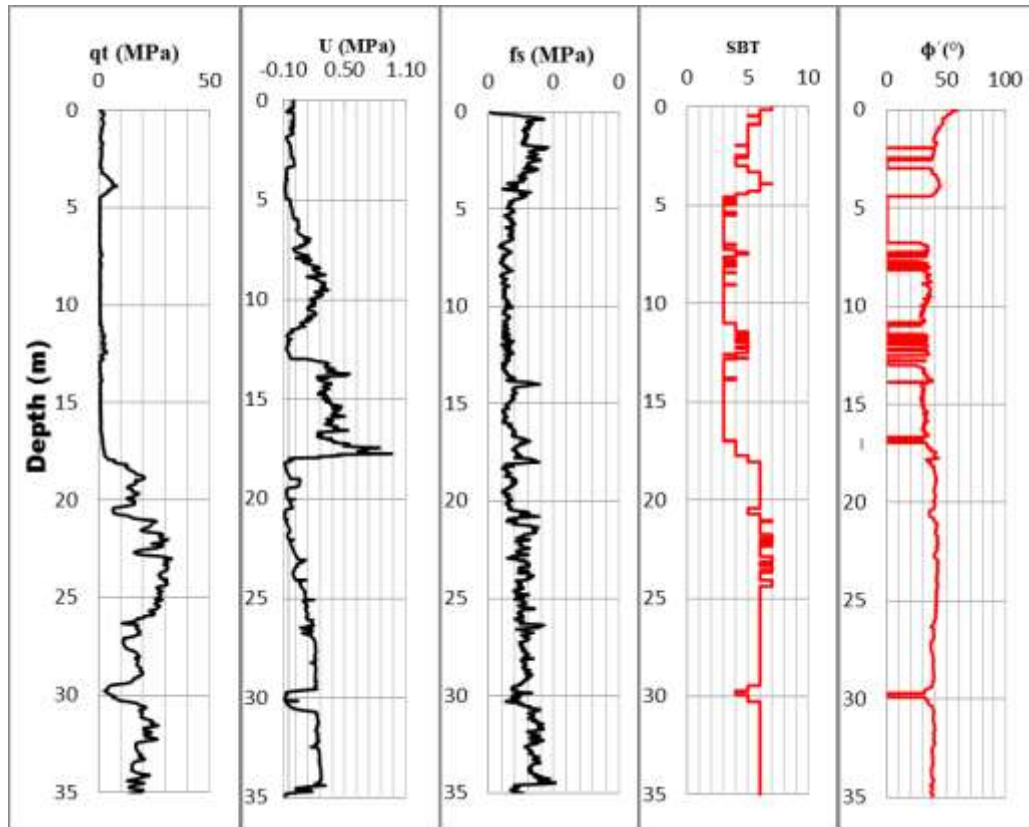
Depth[m]		Ic Average	SBT			
-0.55	-5.55	2.23	Sand mixtures-silty sand to sandy silt	Es	[MPa]	17
				G0	[MPa]	27
				K	m/s	5E-05
				φ	[°]	33
-5.55	-11.55	3.08	Clays- Silty clay to clay	Es	[MPa]	0
				G0	[MPa]	26
				K	m/s	1E-08
				φ	[°]	19
-11.55	-13.55	2.62	Silt mixtyres-clayey silt to silty calt	Es	[MPa]	15
				G0	[MPa]	41
				K	m/s	2E-07
				φ	[°]	14
-11.55	-17.55	3.21	Clays- Silty clay to clay	Es	[MPa]	0
				G0	[MPa]	40
				K	m/s	3E-09
				φ	[°]	28
-17.55	-35.55	1.71	Sands - clean sand to silty sand	Es	[MPa]	97
				G0	[MPa]	125
				K	m/s	2E-04
				φ	[°]	39

(d) Cptu results and soil profile of U206FEN

Layer	CPTs	Depth[m]		Ic Average	SBT			
1	U204FEN U205FEN U206FEN	 6.432 -0.55	 -1.68 -5.55	2.21	Sand mixtures- silty sand to sandy silt	Es G0 K φ	[MPa] [MPa] m/s [°]	23 36 5E-05 34
2	U204FEN U205FEN U206FEN	0	-2.5	1.89	Alluvial	Es G0 K φ	[MPa] [MPa] m/s [°]	18 23 1E-04 44
3	U204FEN U205FEN U206FEN	 -1.68 -5.55	 -4.5 -11.5	3.05	Clays- Silty clay to clay	Es G0 K φ	[MPa] [MPa] m/s [°]	0.2096 35 8.3E-9 9
4	U204FEN U205FEN U206FEN	-2.5 -4.5	-5 -6	2.49	Silt mixtures- clayey silt to silty clay	Es G0 K φ	[MPa] [MPa] m/s [°]	19 40 2E-06 21
5	U204FEN U205FEN U206FEN	-5 -6 -11.5	-18.5 -18.5 -17	3.19	Clays- Silty clay to clay	Es G0 K φ	[MPa] [MPa] m/s [°]	0.0225 44 3E-09 18
6	U204FEN U205FEN U206FEN	-7 -11.5	-13.5 -13.5	2.60	Silt mixtures- clayey silt to silty clay	Es G0 K φ	[MPa] [MPa] m/s [°]	16 38 2E-06 16
7	U204FEN U205FEN U206FEN	-18.5 -18.5 -17	-35 -35 -35	1.75	Sands- clean sand to silty sand	Es G0 K φ	[MPa] [MPa] m/s [°]	95 125 2E-04 37

(e) Final stratigraphy of section U204-205-206FEN

Figure 4- 2 (a) Geological map of section U204-205-206FEN (b) Profile U205FEN (c) Profile U205FEN (d) Profile U206FEN (e) Final stratigraphy of section U204-205-206FEN

Note: The base level of the presented depths is the ground level at the river side of the embankment.
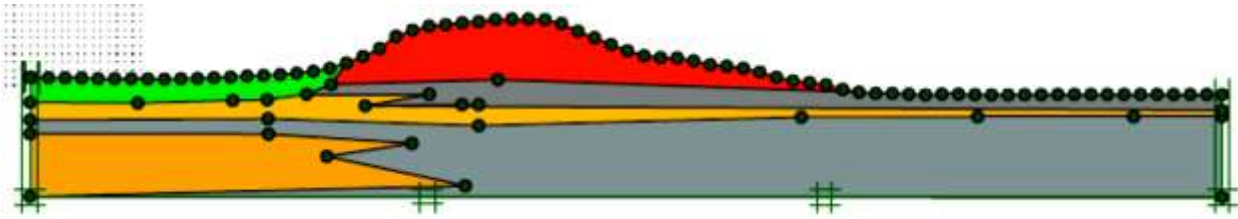
(a) Finite element model of section U204-20-206FEN

(b) Failure mechanism- Low water level- Factor of Safety: 1.802

(c) Failure mechanism- High water level- Factor of Safety: 1.397

Figure 4- 3 (a) Finite element model of section U204-20-206FEN (b) Failure mechanism-
Low water level- Factor of Safety: 1.802 (c) Failure mechanism- High water level- Factor of
Safety: 1.397

(a) Simplified finite element model of section U204-205-206FEN

(b) Failure mechanism- Low water level- Factor of Safety: 1.787

(c) Failure mechanism- High water level- Factor of Safety: 1.402

Figure 4- 4 (a) Simplified finite element model of section U204-205-206FEN (b) Failure mechanism- Low water level- Factor of Safety: 1.787 (c) Failure mechanism- High water level- Factor of Safety: 1.402
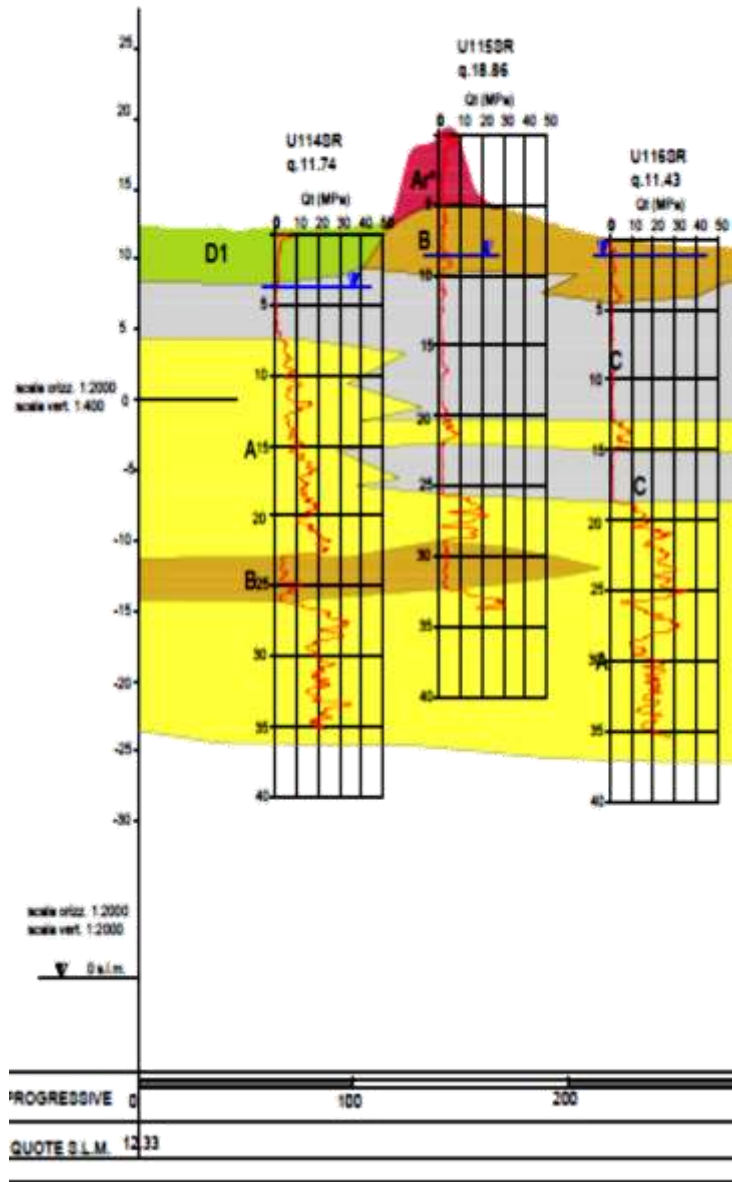
(a) Geological Map of Section U204-205-206FEN
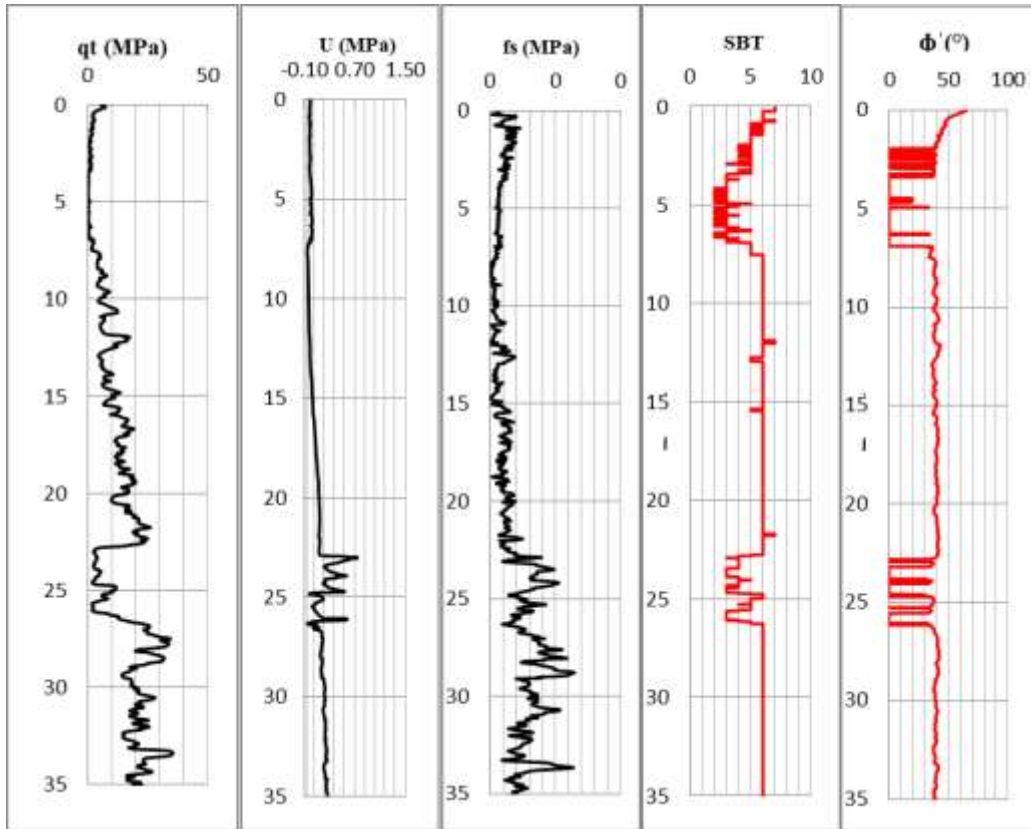
Depth[m]		Ic Average	SBT			
0	-3.5	2.22	Alluvial	Es	[MPa]	16
				G0	[MPa]	23
				K	m/s	6.52E-05
				φ	[°]	36.27231
-3.5	7	3.34	Clay- silty clay to clay	Es	[MPa]	1
				G0	[MPa]	19
				K	m/s	9.82E-09
				φ	[°]	1
7	23	1.65	Sands- clean sand to silty sand	Es	[MPa]	59
				G0	[MPa]	75
				K	m/s	0.000199
				φ	[°]	39
23	26	2.74	Silt mixtures- clayey silt to silty clay	Es	[MPa]	27
				G0	[MPa]	107
				K	m/s	1.02E-06
				φ	[°]	16
26	35	1.77	Sands- clean sand to silty sand	Es	[MPa]	144
				G0	[MPa]	181
				K	m/s	6.13E-05
				φ	[°]	40

(a) CPTu results and soil profile of U114SRRN

Depth[m]		Ic Average	SBT			
7.048	0.548	2.30	Sand mixtures-silty sand to sandy silt	Es	[MPa]	22
				G0	[MPa]	30
				K	m/s	1.7E-05
				φ	[°]	35
0.55	-4.452	2.65	Silt Mixture-Clayey Silt to Silty Clay	Es	[MPa]	10
				G0	[MPa]	44
				K	m/s	0
				φ	[°]	10
-4.45	-12.452	3.07	Clays-Silty clay to clay	Es	[MPa]	3
				G0	[MPa]	46
				K	m/s	6.07E-08
				φ	[°]	2
-12.45	-13.952	2.61	Silt Mixture-Clayey Silt to Silty Clay	Es	[MPa]	23
				G0	[MPa]	59
				K	m/s	0
				φ	[°]	15
-13.95	-18.952	3.04	Clays-Silty clay to clay	Es	[MPa]	12
				G0	[MPa]	65
				K	m/s	1.31E-06
				φ	[°]	7
-18.95	-20.952	1.92	Sands-clean sand to silty sand	Es	[MPa]	83
				G0	[MPa]	113
				K	m/s	8.81E-05
				φ	[°]	34
-20.95	-24.952	2.77	Silt Mixture-Clayey Silt to Silty Clay	Es	[MPa]	18
				G0	[MPa]	101
				K	m/s	1.09E-05
				φ	[°]	16
-24.95	35	1.88	Sands-clean sand to silty sand	Es	[MPa]	154
				G0	[MPa]	193
				K	m/s	2.99E-05
				φ	[°]	39

(C) CPTu results and soil profile of U115SRN
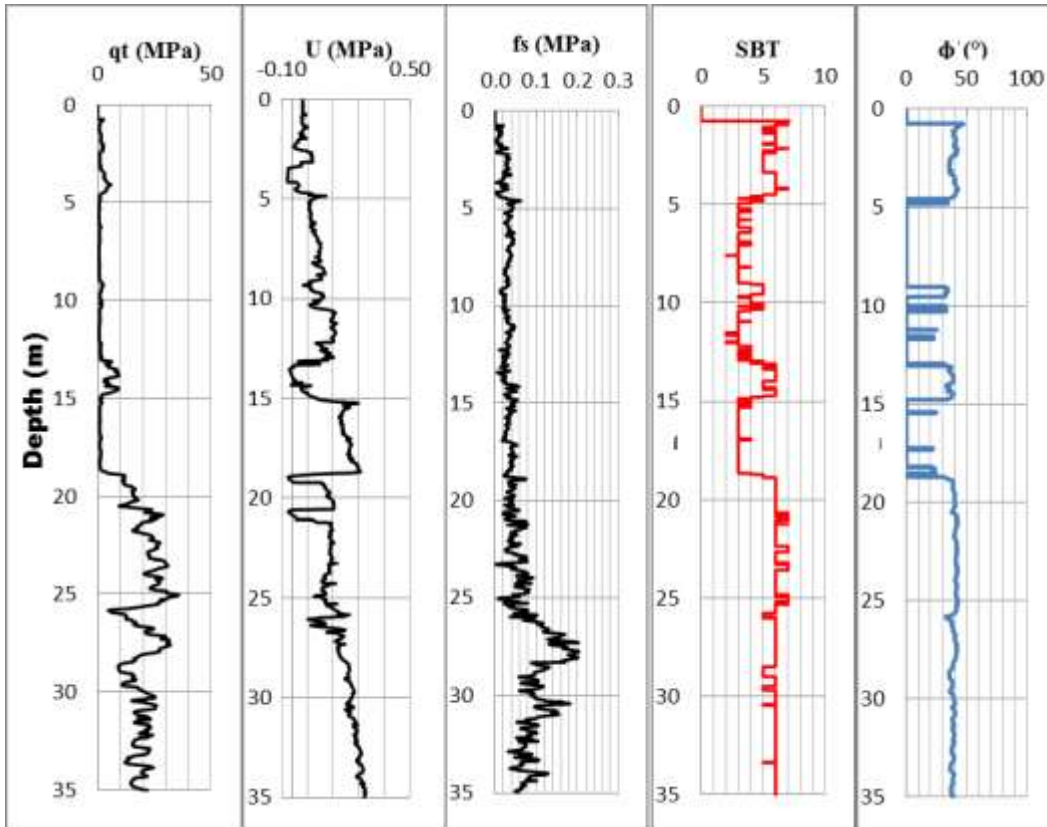
Depth[m]		Ic Average	SBT			
7.048	2.048	2.61	Silt mixtures-clayey silt to silty clay	Es	[MPa]	14
				G0	[MPa]	19
				K	m/s	0.000113
				φ	[°]	37
2.048	-5.952	3.04	Clays-silty clay to clay	Es	[MPa]	2
				G0	[MPa]	30
				K	m/s	5.79E-08
				φ	[°]	3
-5.952	-7.452	1.96	Sands-clean sand to silty sand	Es	[MPa]	47
				G0	[MPa]	59
				K	m/s	3.22E-05
				φ	[°]	37
-7.452	-11.952	3.22	Clays-silty clay to clay	Es	[MPa]	0
				G0	[MPa]	43
				K	m/s	4.3E-09
				φ	[°]	2
-11.952	-11.952	1.69	Sands-clean sand to silty sand	Es	[MPa]	115
				G0	[MPa]	145
				K	m/s	0.00023
				φ	[°]	40

(d) CPTu results and soil profile of 116SRN

Layer	CPTu	Depth[m]		Ic Average	SBT			
1	U114SRN U115SRN U116SRN	7.05	0.55	2.30	Sand mixtures-silty sand to sandy silt	Es G0 K φ	[MPa] [MPa] m/s [°]	22 30 2E-05 35
2	U114SRN U115SRN U116SRN	0.00	-3.50	2.22	Alluvial	Es G0 K φ	[MPa] [MPa] m/s [°]	16 23 7E-05 36
3	U114SRN U115SRN U116SRN	0.55 -0.42	-4.45 -5.42	2.63	Silt mixtures-clayey silt to silty clay	Es G0 K φ	[MPa] [MPa] m/s [°]	12 31 6E-05 23
4	U114SRN U115SRN U116SRN	-3.50 -4.45 -5.42	-7.00 -12.45 -13.44	3.15	Clays-silty caly to clay (2)	Es G0 K φ	[MPa] [MPa] m/s [°]	2 21 4E-08 2
5	U114SRN U115SRN U116SRN	-13.95 -14.92	-18.95 -19.42	3.13	Clays-silty caly to clay	Es G0 K φ	[MPa] [MPa] m/s [°]	6 54 7E-07 5
6	U114SRN U115SRN U116SRN	-23.00 -20.95	-26.00 -24.95	2.68	Silt mixtures-clayey silt to silty clay	Es G0 K φ	[MPa] [MPa] m/s [°]	25 83 7E-07 16
7	U114SRN U115SRN U116SRN	-7.00 -12.45 -13.42	-35.00 -35.00 -35.00	1.80	Sands-clean sand to silty sand	Es G0 K φ	[MPa] [MPa] m/s [°]	90 114 1E-04 38

(e) Final stratigraphy of section U114-115-116SRN

Figure 4- 5 (a) Geological map of section U114-115-116SRN (b) Profile U114SRN (c) Profile U115SRN (d) Profile U116SRN (e) Final stratigraphy of section U114-115-116SRN

Note: The base level of the presented depths is the ground level at the river side of the embankment.
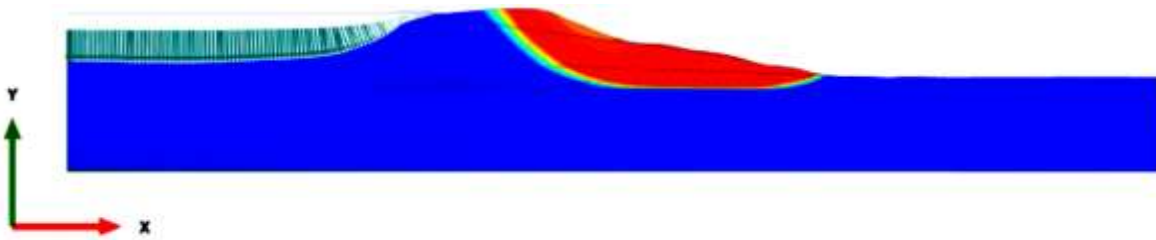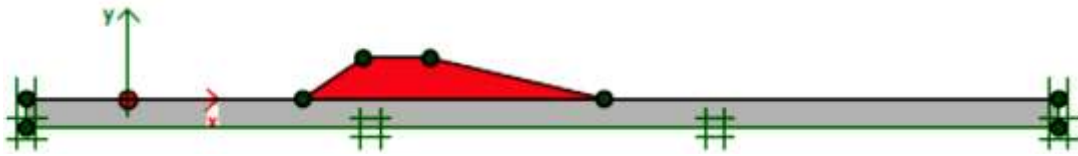
(a) Failure mechanism- Low water level- Factor of Safety: 2.072
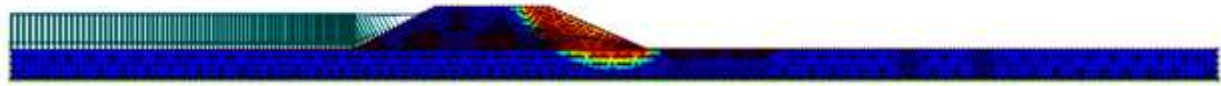
(b) Failure mechanism- High water level- Factor of Safety: 1.881

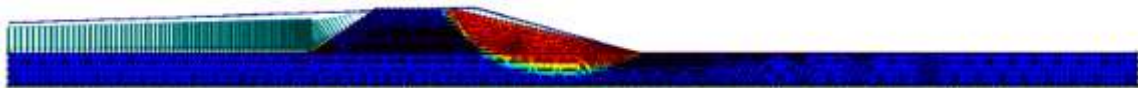Figure 4- 6 (a) Failure mechanism- Low water level- Factor of safety: 2.072 (b) Failure mechanism- High water level- Factor of Safety: 1.881

CHAPTER 5
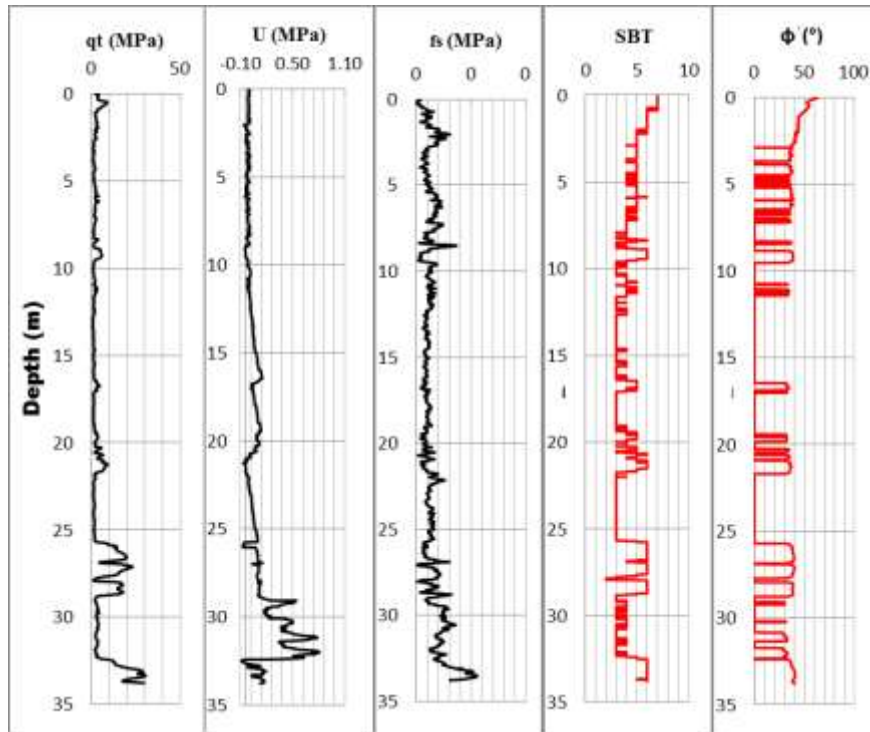# PROPOSED NEURAL NETWORK MODEL FOR SLOPE STABILITY ANALYSIS

5- 1Introduction

In this chapter, an artificial neural network approach is outlined to predict the factors of safety of slopes. The solution is attempted by employing a neural network and predicting the results using the data collected from field case studies.

An artificial neural network can acquire, store, and utilize experiential knowledge like a physical cellular system, to some extent. Neural networks are composed of many simple elements usually operating in parallel (McCullock and Pitts, 1943). The network computation is performed by a dense mesh of com putting nodes and connections. They operate collectively and simultaneously on most or all data and inputs (Minsky, 1954, Minsky and Papert, 1969). The network function is determined largely by the connections between elements. We can train a neural network to perform a particular function by adjusting the values of the connections between elements.

The basic processing elements of neural networks are called artificial neurons, or simply neurons (McCullock and Pitts, 1943; Rosenblatt, 1958). Often we simply call them nodes. Neurons can be perceived as summing and non-linear mapping functions. In some cases they can be considered as threshold units that get activated when their total input exceeds certain bias levels (Rosenblatt, 1958; Widrow and Hoff, 1960). Neurons operate in parallel and are configured in regular architectures. They are often organized in layers, and feedforward and/or feedback connections both within the layer and toward adjacent layers are allowed

(Kohonen, 1977, 1982; Hopfield, 1984). The strength of each connection is expressed by a numerical value called weight, which can be modified.

The most basic characteristic of a neural network is its architecture. Design of network architecture includes selecting the number of layers and the number of nodes in each layer and the interconnection schem es between layers. A variety o f functions can be used as the interconnection function between inputs and hidden layer or between hidden layer and output layer (Kohonen, 1977, 1984; McClelland and Rumelhart, 1986). Neural networks differ from each oher in their learning modes (Widrow and Hoff, 1960). There are a variety of learning rules that establish when and how the connecting weights change. Networks exhibit different speeds and efficiency of learning, thus they also differ in their ability to accurately respond to the values presented at the input (Amari, 1977, 1990; Anderson et al., 1977; Kohonen, 1982, 1988).

A neural network's ability to perform computations is based on the premise that we can reproduce some of the flexibility and power of a human brain by artificial means (Von Neumann, 1958; Arbib, 1987). Advances have been made in applying such systems for problems found intractable or difficult for traditional computation approaches (Kohonen, 1984; Hopfield, 1984; Zurada, 1992). Neural network users do not specify an algorithm to be executed by each computing node (neuron). Instead, they select what in their view is the best architecture, specify the characteristics of the neurons and initial weights, and choose a training mode for the network (Rumelhart et al., 1986; Hertz et al., 1991; Demuth and Beale, 1995, 2000).

Appropriate inputs are then applied to the network so that it can acquire know ledge from the environment. As a result of such exposure, the network assimilates information that can be later recalled by the user (Kohonen, 1988).

The field of neural networks has a history of some six decades but has found meaningful applications only in the past twenty years. The field is still developing rapidly. Today neural networks can be trained to solve problems that are difficult for conventional computational, physics-based methods (Demuth and Beale, 1995, 2000). Neural networks are becoming a useful tool for industry, education and research, a tool that helps users find what works and what does not, and a tool that helps develop and extend the field of neural networks (Zurada, 1992). However, the neural network modeling is limited to the fact that it is based on the data available and extrapolation might not be reliable.

Application of artificial neural network to slope stability analysis is a relatively new topic. It has been well known that neural network can be used to solve both linear and especially non-linear problems. For the case of slope stability, the problem is known to be highly non-linear and a non-linear model may be warranted.

A brief introduction to concepts of artificial neural systems such as artificial neuron model and network architectures is in chapter 3.

5- 2 Modeling Slope Stability with Neural Network

One of the most widely used ANN models in literature are multilayer perceptron network (MLP). MLP is a class of ANN structures using feedforward architecture. The MLP networks are usually applied to perform supervised learning tasks, which learning process is achieved by adjusting the weights in network until a particular input leads to a specific target output. They are usually trained with a back propagation (BP) (Rumelhart et al., 1986) algorithm. Figure 5-1 shows a schematic diagram of a back-propagation neural network. Multilayer perceptron networks consist of an input layer, at least one hidden layer of neurons, and an output layer.

Each of these layers has several processing units, and each unit is fully interconnected with weighted connections to units in the subsequent layer. Each layer contains a number of nodes (Alavi et al., 2010).

Every input is multiplied by each of the nodes using its interconnection weight. The output (*hj*) is obtained by passing the sum of the product through an activation function as follows:

$$h_j = f\left(\Sigma_i x_i w_{ij}\right) \tag{5-1}$$

where $f(\ )$ is activation function, x_i is the activation of *i*th hidden layer node, and w_{ij} is the weight of the connection joining the *j*th neuron in a layer with the *i*th neuron in the previous layer. For nonlinear problems, the sigmoid functions (Hyperbolic tangent sigmoid or log-sigmoid) are usually adopted as the activation function (Alavi et al., 2010). Adjusting the interconnections between layers will reduce the following error function:

$$E = \frac{1}{2}\Sigma_n \Sigma_k (t_k^n - h_k^n)^2 \tag{5-2}$$

where t_k^n and h_k^n are the calculated output and the actual output value, respectively; n is the number of sample, and k is the number of output nodes. Further details of MLPs can be found in Haykins (1999) and Cybenko (1989).
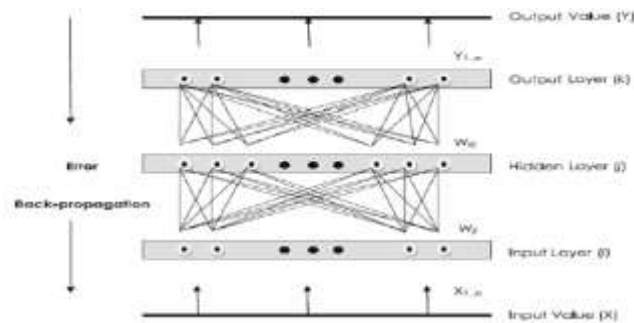
Figure 5- 1 A schematic diagram of a neural network using BP algorithm (Alavi et al., 2010).

5-2- 1 Formulation of the River Banks Stability

In order to have precise estimations of the FS values, it is considered to be a function of several important parameters as follows:

$$FS = f(BC, H1, H2, `1, `2, \phi_1, \phi_2)$$ (5-3)

Where,

BC: Crest width

H1: Embankment height

H2: Height of the first layer under the embankment

HW: Height of the water level

`1: Right hand side slope

`2: Left hand side slope

ϕ'_1: Friction angle of embankment body

ϕ'_2: Friction angle of first layer

The significant influence of the above parameters in determining FS is well understood. Figure 5-2 presents a schematic representation of slop along with the considered parameters.
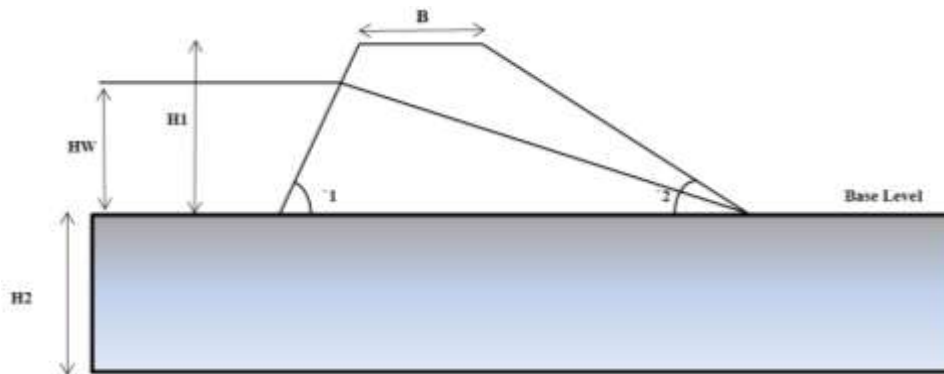
Figure 5- 2 A schematic representation of the investigated slopes

5-2- 2 Model Development Using MLP

The available databases are used for establishing the MLP prediction models. After developing different models with different combinations of the input parameters, the final explanatory variables (BC, H1 H2, HW, `1, `2, $\emptyset'_1$, $\emptyset'_2$) are selected as the inputs of the optimal models. For the development of the MLP models, a script is written in the MATLAB environment using Neural Network Toolbox 5.1 (MathWorks, 2007; Mollahasani et al, 2011). The performance of an ANN model mainly depends on the network architecture and parameter settings. According to a universal approximation theorem (Cybenko, 1989), a single hidden layer network is sufficient for the traditional MLP to uniformly approximate any continuous and nonlinear function. Choosing the number of the hidden layers, hidden nodes, learning rate, epochs, and activation function type plays an important role in the model construction. Hence, several MLP network models with different settings for the mentioned characters are trained to reach the optimal configurations with the desired precision (Mollahasani et al, 2011). The written program automatically tries various numbers of neurons in the hidden layer and reports the correlation coefficient (R), root mean squared error (RMSE) and mean absolute percent error (MAPE) values for each model. The models with the highest R and lowest RMSE and MAPE values on the training data sets are chosen as the optimal models. Various training algorithms are implemented for the training of the MLP network such as gradient descent (traingd), Levenberg–Marquardt (trainlm), and resilient (trainrp) back propagation algorithms. The best results are obtained by Levenberg–Marquardt (trainlm) method. Also, log-sigmoid is adopted as the transfer function between the input-hidden and hidden layer-output layers. The model architectures that gave the best results for the formulation of the FS are found to contain:

Low Water Level:

- One invariant input layer, with 8 (n = 8) arguments and a bias term;
- One invariant output layer with 1 node providing the value of FS.
- One hidden layer having 9 (m = 9) nodes.

High Water Level:

- One invariant input layer, with 8 (n = 8) arguments (BC, H1 H2, HW, `1, `2, $\emptyset'_1$, $\emptyset'_2$) and a bias term;
- One invariant output layer with 1 node providing the value of FS.
- One hidden layer having 16 (m = 16) nodes.

The MLP models are built with a learning rate of 0.05 and trained for 1500 epochs.

5-2- 3 Data Preprocessing

As noted previously, the data used for constructing the model are from The FE stability analysis with Plaxis and steady state seepage analysis on each section of Po river embankments for low and high water level in river. The descriptive statistics of the data used in this study are also given in Table 5-1.
Data for a total of 77 slopes were collected, as shown in Table 5 -2, with the principal parameters of each slope listed. The body of emabankments typically composed of sandy and silty soils. The slope heights range from 4.8m to 10.6m.

Table 5- 1 Descriptive statistics of the variables used in the model development

Low Water Level

Parameter	H1	H2	HW	ø´1	ø´2	B	`1	`2	FS
Mean	7.9	6.4	-1.3	34.2	19.5	10.6	24.2	14.8	1.5
Standard Deviation	1.4	4.2	1.7	6.4	5.9	5.1	6.3	4.2	0.3
Minimum	4.9	2.5	-5.7	19.2	6.3	4.6	8.2	8.3	1.0
Maximum	10.3	28.2	2.3	56.5	38.7	30.0	43.9	27.9	2.3

High Water Level

Parameter	H1	H2	HW	ø´1	ø´2	B	`1	`2	FS
Mean	7.9	6.2	6.8	34.8	20.1	11.3	23.5	14.4	1.3
Standard Deviation	1.5	3.9	1.5	6.5	6.6	6.9	5.3	3.9	0.2
Minimum	4.8	2.5	3.5	23.3	8.8	4.6	13.2	8.3	1.0
Maximum	10.6	28.2	9.2	56.5	41.8	41.6	35.9	26.1	2.1

Table 5- 2 Slopes for Developing the Proposed Artificial Neural Model

No.	SECTION			INPUTS								OUTPUT
				H1	H2	HW	ø´1	ø´2	B	α1	α2	FOS
				m	m	m	°	°	m	°	°	
1	U298RON	U299RON		6	9	-4	23	24	9	29	11	1.358
2				6	9	6	23	24	9	29	11	1.599
3	U295RON	U296RON		7	6	-2	40	15	9	36	11	1.219
4				7	6	6	40	15	9	36	11	1.315
5	U291RON	U292RON	U293RON	7	6	-3	41	26	9	13	12	2.805
6				7	6	6	41	26	9	13	12	1.612
7	U288RON	U289RON	U290RON	8	7	-2	37	26	7	29	9	1.332
8				8	7	8	37	26	7	29	9	1.315
9	U285RON	U286RON	U287RON	10	5	-1	40	27	7	26	15	1.605
10				10	5	8	40	27	7	26	15	1.228
11	U279RON	U280RON	U281RON	10	3	-3	37	27	9	22	11	1.595
12				10	3	9	37	27	9	22	11	1.308
13	U276RON	U277RON	U278RON	10	3	0	35	16	9	27	11	1.232
14				10	3	9	35	16	9	27	11	1.262
15	U273RON	U274RON	U275RON	10	6	-1	29	15	9	32	11	1.019
16				10	6	9	29	15	9	32	11	1.084
17	U270RON	U271RON	U272RON	7	8	-2	40	24	8	21	11	1.819
18				7	8	7	40	24	8	21	11	1.442
19	U264RON	U265RON	U266RON	9	3	-1	40	14	17	31	11	1.052
20				9	3	8	40	14	17	31	11	1.129
21	U262RON	U263RON		8	4	-3	38	24	20	19	11	1.902
22				8	4	7	38	24	20	19	11	1.427
23	U258RON	U259RON	U260RON	10	4	0	39	25	14	26	12	1.231
24				10	4	9	39	25	14	26	12	1.277
25	U258RON	U259RON	U260RON	10	5	0	30	16	26	19	17	1.361
26				10	5	9	30	16	26	19	17	1.102
27	U252RON	U253RON	U254RON	7	5	-3	40	20	16	22	14	1.47
28				7	5	6	40	20	16	22	14	1.121
29	U250FEN	U251FEN		7	9	-2	29	20	10	22	8	1.287
30				7	9	5	29	20	10	22	8	1.213
31	U243FEN	U244FEN		8	4	0	23	33	9	11	10	2.27
32				8	4	7	23	33	9	11	10	1.095

Table 5-2 Continued

No.	SECTION			INPUTS								OUTPUT
				H1	H2	HW	ø´1	ø´2	B	α1	α2	FOS
				m	m	m	°	°	m	°	°	
33	U240FEN	U241FEN	U243FEN	8	5	-2	35	25	8	26	20	1.373
34				8	5	7	35	25	8	26	20	1.161
35	U237FEN	U238FEN	U239FEN	10	5	-1	34	24	12	21	15	1.547
36				10	5	8	34	24	12	21	15	1.362
37	U231FEN	U232FEN	U233FEN	11	6	0	23	16	24	24	11	1.112
38				11	6	9	23	16	24	24	11	1.145
39	U225FEN	U226FEN	U227FEN	9	5	0	28	19	8	25	11	1.208
40				9	5	8	28	19	8	25	11	1.337
41	U222FEN	U223FEN	U224FEN	9	5	1	38	21	8	24	12	1.235
42				9	5	7	38	21	8	24	12	1.256
43	U216FEN	U217FEN	U218FEN	5	7	-4	38	16	6	27	13	1.148
44				5	7	2	38	16	6	27	13	1.008
45	U207FEN	U208FEN	U209FEN	9	3	-2	40	25	8	23	12	1.52
46				9	3	6	40	25	8	23	12	1.283
47	U198FEN	U199FEN	U200FEN	9	4	-1	41	26	5	17	11	2.087
48				9	4	8	41	26	5	17	11	1.565
49	U193FEN	U194FEN		9	6	0	40	16	8	22	11	1.126
50				9	6	8	40	16	8	22	11	1.022
51	U183FEN	U184FEN	U185FEN	9	3	1	33	14	8	24	11	1.078
52				9	3	8	33	14	8	24	11	1.149
53	U168FEN	U169FEN	U170FEN	8	4	-2	36	42	10	25	17	1.585
54				8	4	6	36	42	10	25	17	1.508
55	U165FEN	U166FEN	U167FEN	8	6	-2	23	7	16	16	13	Fail
56				8	6	6	23	7	16	16	13	Fail
57	U162FEN	U163FEN	U164FEN	8	6	-2	33	20	7	18	13	1.632
58				8	6	7	33	20	7	18	13	1.202
59	U156FEN	U157FEN	U158FEN	8	6	-2	40	24	21	12	9	2.7
60				8	6	7	40	24	21	12	9	1.56
61	U153FEN	U154FEN	U155FEN	6	7	-2	38	6	13	21	19	1.212
62				6	7	5	38	6	13	21	19	FAIL
63	U151FEN	U150FEN	U152FEN	7	7	-3	41	25	10	25	16	1.729
64				7	7	6	41	25	10	25	16	1.492

No.	SECTION			INPUTS								OUTPUT
				H1	H2	HW	ø´1	ø´2	B	α1	α2	FOS
				m	m	m	°	°	m	°	°	
65	U147FEN	U148FEN	U149FEN	5	7	N.A	37	19	9	28	22	1.195
66				5	7	4	37	19	9	28	22	0.983
67	U144FEN	U145FEN	U145FEN	7	6	-3	31	15	8	30	14	1.24
68				7	6	7	31	15	8	30	14	1.19
69	U141FEN	U142FEN	U143FEN	7	7	2	37	17	10	33	15	1.244
70				7	7	7	37	17	10	33	15	1.321
71	U138FL	U139FL	U140FL	8	8	0	29	24	7	27	19	1.465
72				8	8	8	29	24	7	27	19	1.38
73	U132FL	U133FL	U134FL	9	6	-1	33	25	7	30	14	1.482
74				9	6	8	33	25	7	30	14	1.652
75	U129FL	U130FL	U131FL	8	3	1	38	34	10	27	24	1.904
76				8	3	7	38	34	10	27	24	FAIL
77	U127FL	U128FL		7	7	-3	38	14	5	24	18	2.375
78				7	7	5	38	14	5	24	18	2.16
79	U123FL	U124FL	U125FL	9	5	-1	35	30	8	25	15	1.955
80				9	5	8	35	30	8	25	15	1.946
81	U120S RN	U121S RN	U122S RN	8	3	-2	39	12	13	29	28	1.157
82				8	3	7	39	12	13	29	28	FAIL
83	U114S RN	U115S RN	U116S RN	7	5	-2	35	23	20	28	24	2.072
84				7	5	6	35	23	20	28	24	1.881
85	U111S RN	U112S RN	U113S RN	8	9	-1	35	15	13	24	26	1.274
86				8	9	7	35	15	13	24	26	1.043
87	U105S RN	U106S RN	U107S RN	5	7	-4	41	16	6	26	17	1.612
88				5	7	3	41	16	6	26	17	1.415
89	U100S RN	U101S RN		9	4	-2	35	15	5	25	17	1.303
90				9	4	8	35	9	5	25	17	1.083
91	U97CP	U98CP	U99CP	8	11	1	38	15	6	32	15	1.125
92				8	11	7	38	15	6	32	15	1.138
93	U94CP	U95CP	U96CP	7	8	-2	29	14	5	18	18	1.507
94				7	8	6	29	14	5	18	18	1.072
95	U91CP	U92CP	U93CP	8	5	-1	37	17	6	14	19	1.178
96				8	5	7	37	17	6	14	19	1.24

Table 5-2 Continued

No.	SECTION			INPUTS								OUTPUT
				H1	H2	HW	ø´1	ø´2	B	α1	α2	FOS
				m	m	m	°	°	m	°	°	
97	U89CP	U90CP		9	7	0	27	20	11	32	18	1.179
98				9	7	8	27	10	11	32	18	1.304
99	U85CP	U86CP	U87CP	10	4	2	34	17	8	27	16	1.23
100				10	4	9	34	10	8	27	16	1.122
101	U52GSN	U53GSN	U54GSN	8	4	2	25	20	11	14	19	1.509
102				8	4	7	25	20	11	14	19	1.287
103	U49GSN	U50GSN	U51GSN	7	28	2	24	39	5	21	8	1.772
104				7	28	6	24	39	5	21	8	2.082
105	U46GSN	U47GSN	U48GSN	6	3	1	26	10	30	23	16	1.048
106				6	3	5	26	7	30	23	16	FAIL
107	U40GSN	U41GSN	U42GSN	5	5	-2	38	13	7	19	18	1.586
108				5	5	5	38	13	7	19	18	1.167
109	U34GL	U35GL	U36GL	7	12	-4	23	10	7	30	15	1.14
110				7	12	6	23	10	7	30	15	1.083
111	U31GL	U32GL	U33GL	7	7	-2	41	19	17	22	17	1.892
112				7	7	6	41	19	17	22	17	1.45
113	U25GL	U26GL	U27GL	7	6	-6	38	20	6	19	11	2.121
114				7	6	6	38	20	6	19	11	1.61
115	U22GL	U23GL	U24GL	7	6	-1	39	20	10	21	15	1.888
116				7	6	5	39	20	10	21	15	1.546
117	U19BR	U20BR	U21BR	7	6	-1	32	26	9	21	14	2.117
118				7	6	-9	32	26	9	21	14	1.825
119	U16BR	U17BR	U18BR	8	8	-3	24	20	17	14	19	1.743
120				8	8	7	24	20	17	14	19	1.29
121	U13BR	U14BR	U15BR	7	7	-3	57	14	9	20	12	1.738
122				7	7	6	57	14	9	20	12	1.233
123	U07BR	U08BR	U09BR	5	8	-1	40	15	42	23	11	1.684
124				5	8	4	40	15	42	23	11	1.47
125	U04BR	U05BR	U06BR	6	7	-1	32	22	10	18	17	2.145
126				6	7	5	32	22	10	18	17	1.583
127	U01BR	U02BR	U03BR	6	4	-1	35	20	8	22	13	1.843
128				6	4	5	35	20	8	22	13	1.56

No.	SECTION			INPUTS								OUTPUT
				H1	H2	HW	ø´1	ø´2	B	α1	α2	FOS
				m	m	m	°	°	m	°	°	
129	U28CAMPAGNA			8	3	0	43	19	12	30	9	1.436
130				8	3	7	43	8	12	30	9	1.699
131	U26ARGINE			10	21	-3	30	13	9	21	11	1.269
132				10	21	9	30	13	9	21	11	1.024
133	U234FEN	U236FEN		6	7	-1	35	21	9	44	15	1.298
134				6	7	4	35	21	9	44	15	1.381
135	U219FEN	U220FEN	U221FEN	8	3	-1	35	16	20	26	24	1.324
136				8	3	6	35	16	20	26	24	1.134
137	U22ARGINE			9	7	-4	31	18	5	14	14	2.083
138				9	7	7	31	18	5	14	14	1.306
139	U213FEN	U214FEN	U215FEN	10	5	0	19	12	8	8	11	1.407
140				10	5	7	19	6	8	8	11	FAIL
141	U204FEN	U205FEN	U206FEN	9	6	1	34	19	15	34	13	1.787
142				9	6	6	34	19	15	34	13	1.402
143	U201FEN	U202FEN	U203FEN	6	7	-3	39	24	9	27	14	1.978
144				6	7	3	39	24	9	27	14	1.865
145	U25ARGINE			5	8	-14	31	26	14	24	22	2.011
146				5	8	4	31	26	14	24	22	1.672
147	U189FEN	U190FEN	U191FEN	7	6	-3	43	30	7	27	9	2.316
148				7	6	5	43	30	7	27	9	2.381
149	U186FEN	U187FEN	U188FEN	8	3	-3	27	26	9	25	11	1.676
150				8	3	7	27	26	9	25	11	1.793
151	U177FEN	U178FEN	U179FEN	5	14	-3	40	26	9	28	12	1.491
152				5	14	5	40	26	9	28	12	1.449
153	U172FEN	U173FEN		8	4	-2	36	19	9	14	21	1.739
154				8	4	8	36	19	9	14	21	1.109

For the MLP analysis, the data sets were randomly divided into training and testing subsets. Training data were used for learning. The testing data were used to measure the performance of the MLP models on data that played no role in building the models (Alavi et al., 2010). Out of the available data for the low level, 44 and 14 data vectors are used for the training and testing, respectively. For the high water level, 32 data vectors are used for the training process and 11 data are taken for the testing of the models. In order to obtain a consistent data division, several combinations of the training and testing sets are considered. Both the input and output variables are normalized in this study. After controlling several normalization methods (Mollahasani et al, 2011; Mesbahi, 2000), the following method is used to normalize the variables to a range of [L, U]:

$$X_n = ax + b \qquad (5\text{-}4)$$

Where,

$$a = \frac{U - L}{X_{max} - X_{min}} \qquad (5\text{-}5)$$

$$b = U - aX_{max} \qquad (5\text{-}6)$$

in which X_{max} and X_{min} are the maximum and minimum values of the variable and X_n is the normalized value. In the present study, $L = 0.05$ and $U = 0.95$.

Comparisons of the predicted versus experimental FS values for the low and high water levels are shown in Figures 5-3 and 5-4, respectively.
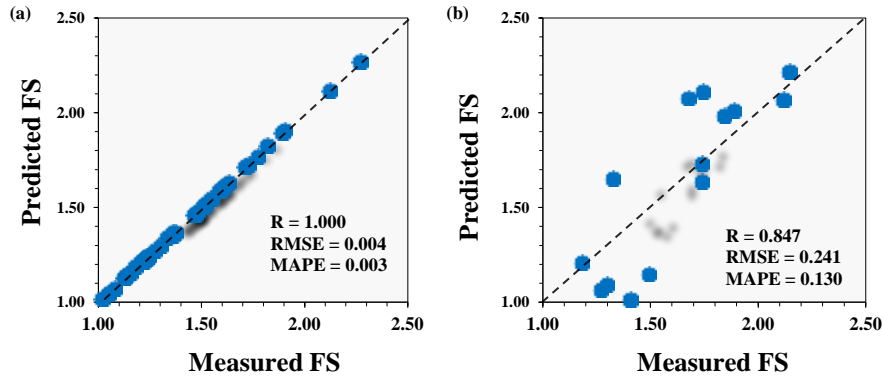
Figure 5- 3 Predicted versus experimental FS values using for low water level: (a) training data, (b) testing data
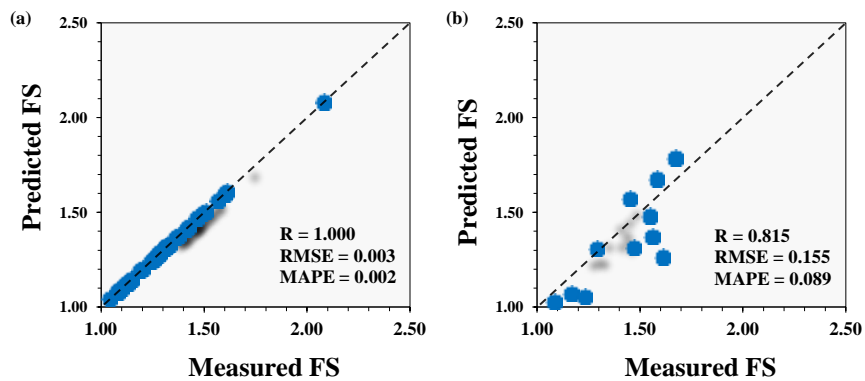

Figure 5- 4 Predicted versus experimental FS values using for high water level: (a) training data, (b) testing data

5- 3 Performance Analysis of the Models

Precise models are developed for the prediction of FS upon reliable databases. Based on a logical hypothesis (Smith, 1986), if a model gives R > 0.8, and the RMSE and MAPE values are at the minimum, there is a strong correlation between the predicted and measured values. The model can therefore be judged as very good. It can be observed from Figures 5 and 6 that the ANN models with high R and low RMSE and MAPE values are able to predict the target values to an

acceptable degree of accuracy. The performance of the models on the training data is much better than that on the testing data. Moreover, the predictions for the low water level are more accurate than those for the high water level. No rational model has been found for the prediction of FS that encompasses the influencing variables considered in this study. Thus, it is not possible to conduct a comparative study between the results of this research and those in hand. However, a multivariable linear least squares regression (LSR) analysis is performed to have an idea about the predictive power of the best MLP models. The LSR prediction equations relate FS to the predictor variables as follows:

$$FS = \alpha_1 BC + \alpha_2 H1 + \alpha_3 H2 + \alpha_4 HW + \alpha_5 `1 + \alpha_6 `2 + \alpha_7 \phi_1 + \alpha_8 \phi_2 + \alpha_9 \qquad (5\text{-}7)$$

where α denotes coefficient vector. The LSR model is calibrated using the entire databases for the high and low water level. Eviews software package is used to perform the regression analysis. The LSR-based formulations of FS are as given below:

High Water Level:

$$FS = -0.0444 BC + 0.0092 H1 + 0.0171 H2 - 0.00059 HW + \\ 0.0179`1 + 0.00042`2 + 0.0046 \phi_1 - 0.0106 \phi_2 + 1.67404 \qquad (5\text{-}8)$$

Low Water Level:

$$FS = -0.0525 BC - 0.0045 H1 + 0.0289 H2 + 0.00546 HW + \\ 0.0293`1 + 0.00018`2 + 0.0239 \phi_1 + 0.00608 \phi_2 + 1.5702 \qquad (5\text{-}9)$$

A comparison of the predictions made by the MLP and LSR models and the measured FS values is shown in Figure 5-5. It is obvious that, in all cases, the MLP models have a remarkably better performance than the LSR models. Empirical modeling based on statistical regression techniques has significant limitations. Most commonly used regression analyses can have large uncertainties. It has own major drawbacks pertaining idealization of complex processes, approximation and averaging widely varying prototype conditions. Contrary to MLP, the regression-based methods model the nature of the corresponding problem by a pre-defined linear or nonlinear equation (Mollahasani et al., 2011).
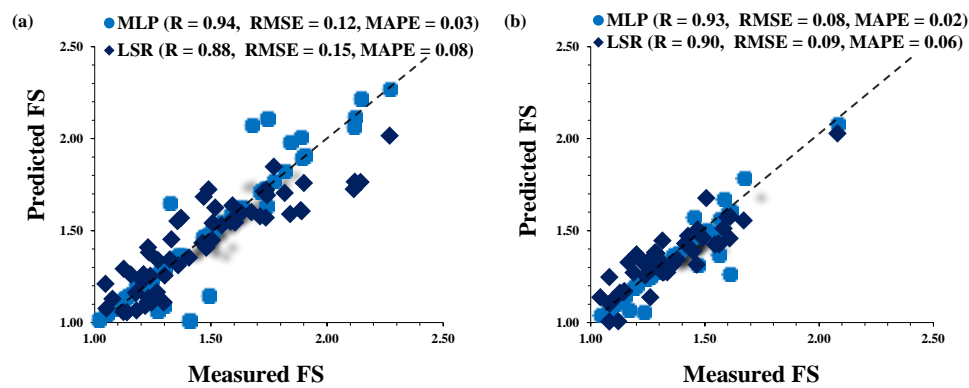

Figure 5- 5 A comparison of the predictions made by the MLP and LSR models: (a) Low water level (b) High water level

5- 4 Conclusions

In this research, reliable models are derived for assessing the stability analysis of river banks along the Po River in Italy using the ANN paradigm. The FS of slopes along the river is formulated in terms of several influencing variables. The developed models for both high and low water levels give reliable estimations of the FS values and outperform the regression-based models. The models can be improved to make more accurate predictions for a wider range by adding newer data sets for other soil types and test conditions. A major distinction of ANN for determining the FS values lies in its powerful ability to model the mechanical behavior without assuming prior form of the existing relationships.

CHAPTER 6
CONCLUSION

6- 1Summary

This research attempts to evaluate slope instability using the BPNN model combined with a detailed field survey. In this study, a literature review of the slope stability analysis methods (Chapter 2) were introduced and followed by a description of artificial neural networks and its application in geotechnical engineering (Chapter 3). Collecting a comprehensive geotechnical database from CPTu test and FE stability analysis on 77 Po river banks with a description of the study site is presented in chapter4.

In Chapter5, an artificial neural network model is introduced, as an alternate approach, for modeling slope stability. Out of the available data for the low level, 44 and 14 data vectors are used for the training and testing, respectively. For the high water level, 32 data vectors are used for the training process and 11 data are taken for the testing of the models. In order to obtain a consistent data division, several combinations of the training and testing sets are considered. The available databases are used for establishing the MLP prediction models. After developing different models with different combinations of the input parameters, the final explanatory variables (BC, H1 H2, HW, `1, `2, $\emptyset´_1$, $\emptyset´_2$) are selected as the inputs of the optimal models. According to a universal approximation theorem (Cybenko, 989), a single hidden layer network is sufficient for the traditional MLP to uniformly approximate any continuous and nonlinear function. The written program automatically tries various numbers of neurons in the hidden layer and reports the correlation coefficient (R), root mean squared error (RMSE) and mean absolute percent error (MAPE) values for each model. The best results are obtained

by Levenberg–Marquardt (trainlm) method. Also, log-sigmoid is adopted as the transfer function between the input-hidden and hidden layer-output layers. The MLP models are built with a learning rate of 0.05 and trained for 1500 epochs. Also a multivariable linear least squares regression (LSR) analysis is performed to have an idea about the predictive power of the best MLP models, in comparison with a classical statistical approach.

6- 2 Conclusions and Recommendations

1. The proposed ANN model is found to be more effective in representing relatively complex slopes with layered soils and/or pore water pressures. it is worth recognizing that the BPNN, as an effective approach of evaluation methods for slope stability, represents a method with huge potential for application in geotechnical engineering.

2. A comparison of the predictions made by the MLP and LSR models and the measured FS values illustrates that the MLP models have a remarkably better performance than the LSR models.

3. The models can be improved to make more accurate predictions for a wider range by adding newer data sets for other soil types and test conditions.

4. The study also pointed out that the main criticism of the ANN methodology is its inability to trace and explain the logic it uses to arrive at the outputs from the inputs.

5. It should be noted, however, that the application of BPNN to slope-stability analysis is based on the assumption that the training data sets have the similar mechanisms and are based on similar geological conditions.

6. Based on the method of slices, numerous traditional simplified deterministic methods for FS calculation suffer from limitations, such as the inability to

consider variability in input parameters. However, other methods cannot be substituted for the deterministic approach to slope engineering.

7. The database developed in this study, having data for 77 slopes including field data, is found to be adequate for training the proposed ANN model. Additional field data would enrich the database further.

8. The factors of safety obtained by the proposed ANN model are in general agreement with the results from the FEM analyses.

9. This study illustrates that the proposed ANN model is useful alternatives for slope stability analyses. Other techniques such as finite element method can be used for a more detailed analysis when needed.

10. Artificial neural network is still very much a developing field. It is, therefore, necessary for the potential users of this new tool (i.e. neural network technique) to be well aware of the assumptions underlying the technique as well as of its limitations. One must, therefore, be wary of attaching overwhelming importance to the absolute values of calculated factors of safety. It is the comparison of calculated factors of safety using different alternatives that is really important. These thoughts should be kept well in mind when adopting any analyses of slope stability.

11. As to the neural network-based approach, further study should involve collecting more field data that can be used to enhance training and evaluation of the model. Also, future studies should account for the effect of pore water pressure in a more comprehensive manner including the time dependent nature of pore pressure and slope failure.

12. The principal component analysis and ranking of input factors used in developing the neural network model are also considered important topics for future research.

13. Laboratory and field studies can be pursued to generate data that can be used for further development and validation of neural network models.

REFERENCES

Abramson L. W. (1996), Slope Stability and Stabilization Methods. Wiley, New York.

Abramson, L. W., Lee, T. S., Sharma, S., and Boyce, G. M. (2002). Slope Stability Concepts.

Abu-Kiefa, M. A. (1998). "General regression neural networks for driven piles in cohesionless soils." Journal of Geotechnical & Geoenviromental Engineering, ASCE, 124(12), 1177-1185.

Alavi, A.H., Gandomi, A.H., Mollahasani, Ali., Heshmati, A.A. & Rashed, A. 2010. Modeling of maximum dry density and optimum moisture content of stabilized soil using artificial neural networks. J. Plant Nutr. Soil Sci., 173, 368–379. DOI: 10.1002/jpln.200800233.

Amari S. I. (1990), Mathem atical Foundations of Neurocom puting. IEEE Proc. 78(9): 1443-1463.

Amari S. I. (1977), Neural Theory o f Association and Concept Formation. Biol. Cybem . 26: 175-185.

Amari, S. I., Murata, N., Muller, K. R., Finke, M., and Yang, H. H. (1997). "Asympotic statistical theory of overtraining and cross-validation." IEEE Transactions on Neural Networks, 8(5), 985-996.

Anderson J. A., Silverstein J. W ,, Rite S. A. and Jones R. S. (1977), Distinctive Features. Categorical Perception, and Probability Learning: Some Applications of a Neural Model. Psych. Rev. 84: 413-451.

Arbib M. A. (1987), Brains, M achines, and M athem atics. 2nded. New York: Springer Verlag. Hopfield J. J. (1984), Neurons with Graded Response Have Collective Computational Properties like Those of Two State Neurons. Proc. Natl. Acad. Sci. 81: 3088-3092.

Behrens, T., Förster, H., Scholten, T., Steinrücken, U., Spies, E.& Goldschmitt, M.2005. Digital soil mapping using artificial neural networks. J. Plant Nutr. Soil Sci. 168, 21–33.

Bishop A.V. (1971). The influence of progressive failure on the choice of the method of stability analysis. Geotechnique,V21, pp.168-172.

Bishop, A. W. (1955). The use of slip circles in stability analysis of slopes. Geotechnique, Vol. 5 No. 1, pp. 7-17.

Brown, M., and Harris, C. J. (1994). Neurofuzzy adaptive modeling and control, Prentice-Hall, Englewood Cliffs, New Jersey.

Chester, D. L. (1990). "Why two hidden layers are better than one." International Joint Conference on Neural Networks, 1, 265-268.

Ching R. K. H. and Fredlund D. G. (1983), Some difficulties associated with the limit equilibrium method of slices. Can. Geotech. J. 20(4), 661-672.

Chollada, K. & Chub-uppakarn, Tanan. 2013. 18th National Convention on Civil Engineering. Chiang Mai, Thailand.

Costa F. L. M. and Thomas J. E. S. (1984), Stability analysis of slopes in soils with non-linear strength envelopes using non-circular slip surfaces. International Symposium on Landslides, pp. 393-397.

Dai F. C., Chen S. Y. and Li Z. F. (2000), Analysis of landslide initiative mechanism based on stress-strain behavior of soil. Chinese Journal of Geotechnical Engineering, Vol. 22, No. 1, p. 127-130.

Davis E. H. (1968), Theories of plasticity and the failure of soil masses. Soil Mechanics Selected Topics (Ed. I.K.Lee), Butterworths, London, pp. 341 - 380.

Dayakar, P.& Rongda, Z. 1999. Triaxial compression behavior of sand and gravel using artificial neural networks (ANN). Comput Geotech. 24, 207–230.

Demuth H. and Beale M. (1995), Neural Network Toolbox for Use with MATLAB. The Math Works Inc., Natick, Mass.

Demuth H. and Beale M. (2000), Neural Network Toolbox for Use with MATLAB. The Math Works Inc., Natick, Mass.

El-Naggar, Mohamed. 2010. Enhancement of steel sheet-piling quay walls using grouted anchors. Soil Science and Environmental Mnagement. 1(4),69-76.

Eslaamizaad, S., and Robertson, P.K. 1996b. Cone penetration test to evaluate bearing capacity of foundation in sands. In Proceedings of the 49th *Canadian Geotechnical Conference*. St John's, Newfoundland. September, pp. 429-438.

Eslaamizaad, S. and Robertson, P.K., 1997. Evaluation of settlement of footings on sand from seismic in-sity tests. *In Proceedings of the 50th Canadian Geotechnical Conference*, Ottawa, Ontario, October 1997, Vol.2, pp. 755-764.

Flood, I. (1991)."A Gaussian-based neural network architecture and complementary training algorithm." Proceedings of the International Joint Conference on Neural Networks, New York, 171-176.

Flood, I., and Kartam, N. (1994). "Neural networks in civil engineering I: Principles and understanding." Journal of Computing in Civil Engineering, 8(2), 131-148.

Garson, G. D. (1991). "Interpreting neural-network connection weights." AI Expert, 6(7), 47-51.

Goh, A. T. C. (1994a). "Nonlinear modeling in geotechnical engineering using neural networks." Australian Civil Engineering Transactions, CE36(4), 293-297.

Goh, A. T. C. (1994b). "Seismic liquefaction potential assessed by neural network." Journal of Geotechnical & Geoenvironmental Engineering, ASCE, 120(9), 1467-1480.

Griffiths, D.V. & Lane, P.A. 1999. Slope stability analysis by finite elements. Geotechnique 49(3): 387-403.

Hertz J.A. and Palmer R.G. (1991), Introduction to the Theory of Neural Computation. Redwood City, Calif.: Addison-Wesley Publishing Co.

Huat, A. R. 2006. Stability Analysis and Stability Chart for Unsaturated Residual Soil Slope, American Journal of Environmental Sciences 2, pp. 154-160.

Janbu, N. (1957). Earth pressure and bearing capacity calculations by generalised procedure of slices. Proceedings of the 4th International Conference, SMFE, London, 2, pp. 207-12.

Janbu, N. (1973). Slope Stability Computations. Embankment Dam Engineering, Casagrande Volume, pp. 47-86.

Jefferies, M.G., and Davies, M.P., 1993. Use of CPTU to estimate equivalent SPT N60. *Geotechnical Testing Journal*, ASTM, **16**(4): 458-468.

Jiao Y. Y., Ge X. R., Liu Q. S. and Feng S. R. (2000), Three-dimensional discrete element method and its application in landslide analysis. Chinese Journal of Geotechnical Engineering, Vol. 22, No. 1, p. 101-104.

J. M. Duncan, A. L. Buchignani and M. De Wet, "An Engineering Manual for Slope Stability Studies," Virginia Polytechnic Institute, Blacksburg, 1987.

J. M. Duncan, "State of the Art: Limit Equilibrium and Finite-Element Analysis of Slopes," Journal of Geotechnical Engineering, Vol. 122, No. 7, 1996, pp. 577-596. doi:10.1061/(ASCE)0733-9410(1996)122:7(577)].

Kohonen T. (1977), Associative Memory: A System-Theoretical Approach, Berlin Springer-Verlag.

Kohonen T. (1982), A Simple Paradigm for the Self-Organized Formation of Structured Feature Maps. Competition and Cooperation in Neural Nets. ed.

Kohonen T. (1984), Self-Organization and Associative Memory. Berlin: Springer- Verlag.

Kohonen T. (1988), The Neural' Phonetic Typewriter. IEEE Computer27(3): 1 1-22.

Krahn, J. (2004). Stability Modelling with SLOPE/W. An Engineering Methodology, Published by GeoSlope International.

Kulhawy, F.H., and Mayne, P.H., 1990. *Manual on estimating soil properties for foundation design*, Report EL-6800 Electric Power Research Institute, EPRI, August 1990.

Lapedes, A., and Farber, R. (1988). "How neural networks work." Neural Information Processing Systems, American Institute of Physics, 442-456.

Lee, I. M., and Lee, J. H. (1996). "Prediction of pile bearing capacity using artificial neural networks." Computers and Geotechnics, 18(3), 189-200.

Maier, H. R., and Dandy, G. C. (2000). "Neural networks for the prediction and forecasting of water resources variables: A review of modeling issues and applications." Environmental Modeling & Software, 15(2000), 101-124.

Marchi, E. 1994. Hydraulic aspects of the Po River flood occurred in 1951, in: Proceedings of the XVII Conference on Historical Studies, Rovigo, 2–24 November 1991, Minnelliana Editions, Rovigo (in Italian).

Masters, T. (1993). Practical neural network recipes in C++, Academic Press, San Diego, California.

Matsui, T. & San, K-C. 1992. Finite element slope stability analysis by shear strength reduction technique. Soil Found, 32(1):59-70.

Mayne, P.W., 2005. Integrated Ground Behavior: In-Situ and Lab Tests, *Deformation Characteristics of Geomaterials*, Vol. 2 (Proc. Lyon), Taylor & Francis, London, pp. 155-171.

McC lelland T. L., Rumelhart D. E., and the PDP Research Group (1986), Parallel Distributed Processing. Cambridge: The MIT Press.

McCullock W. S. and Pitts W. H. (1943), A Logical Calculus of the Ideas Imminent in Nervous Activity. Bull. M ath. Biophy. 5:115-133.

Minsky M. (1954), Neural Nets and the Brain. Doctoral Dissertation, Princeton University, NJ.

Minsky M. and Papert S. (1969), Perceptrons. Cambridge, Mass.: MIT Press.

Mwasha .2008. Investigating the Effects of Basal Reinforcement on the Critical Slip Circle Parameters of an Embankment on Soft Ground: A Parametric Study, Electronic Journal of Geotechnical Engineering, Vol. 13.

Montanari, A. 2012. Hydrology of the Po River. Hydrology and Earth System Sciences.16:3739–3747, DOI:10.5194/hess-16-3739-2012.

Morgenstem N. (1963), Stability charts for earth slopes during rapid draw down. Geotechnique, V13, pp. 121-131.

Morgenstern, N. R. and Price, V. E. (1965). The Analysis of the Stability of General Slip Surfaces. Geotechnique, Vol. 15, No. 1 pp. 77-93.

Nash, D. (1987). Comprehensive Review of Limit Equilibrium Methods of Stability Analysis. Slope Stability, Chapter 2. M. G. Andersen and K. S. Richards, Eds. New York: Wiley, pp. 11-75.

Nordal, S. and Glaamen, M. G. (2004). Some examples of slope stability evaluations from Norwegian geotechnical practice. Geotechnical Innovations, Edited by Brinkgreve, R. B. J., Schad, H., Schweiger, H. F. and Willand, E., pp. 347-63.

Ozcep., Erol., Saraçolu. & Halilolu.2010. Seismic Slope Stability Analysis: Gurpinar (Istanbul) as a Case History, Scientific Research and Essays Vol. 5, pp. 1615-1631.

Piccoli, A. 1976. The most important floods of the Po River from 1900 to 1970, Accademia Nazionale dei Lincei, Rome (in Italian).

Plaxis 2D 2011, Reference Manual, Delft, Netherlands.

Ripley, B. D. (1996). Pattern recognition and neural networks, Cambridge University Press, Cambridge.

Robertson, P.K., 2009. Interpretation of cone penetration tests – a unified approach. *Canadian Geotechnical Journal,* 46:1337-1355.

Robertson, P.K., 2010. Soil behaviour type from the CPT: an update. *2nd International Symposium on Cone Penetration Testing*, CPT'10, Huntington Beach, CA, USA. www.cpt10.com

Rosenblatt F. (1958), The Perceptron: A Probabilistic Model for Information Storage and Organization in the Brain. Psych. Rev. 65: 386-408.

Rumelhart D. E., Hinton G. E. and William s R. J. (1986), Learning internal representations by error propagation. Parallel Data Processing, MIT Press, Cambridge, pp. 318-362.

Sakellariou, M.G. & Ferentinou, M.D. 2005. A study of slope stability prediction using neural networks. Geotechnical and Geological Engineering. 23: 419–445. DOI 10.1007/s10706-004-8680-5.

S. Amari, M. Arbib. vol. 45. Berlin: Springer-Verlag.

Sarle, W. S. (1994). "Neural networks and statistical models." Proceedings of the 19th Annual SAS Users Group International Conference, Cary, NC: SAS Institute, 1538-1550.

Shahin, M. A., Maier, H. R., and Jaksa, M. B. (2005c). "Investigation into the robustness of artificial neural network models for a case study in civil engineering." Proceedings of the International Congress on Modeling and Simulation, MODSIM 2005, Melbourne (Australia), 79-83.

Sharma, R.K. 2011. Comparative analysis of stability of slopes by limit equilibrium method and software GEO5 and Plaxis 2D. Las Vegas International Academic Conference.

Shioi Y. and Sutoh S. (1999), Collapse of high embankment in the 1994 far-off Sanriku Earthquake. Slope Stability Engineering, Yagi, Yamagami & Jiang, Balkema, Rotterdam, pp.559-564.

SLIDE (2003). Stability analysis for soil and rock slopes. Slide, User's Guide, Geomechanics Software Solutions, Rocscience Inc., Canada. www.rocscience.com.

Slope Stabilisation and Stabilisation Methods, Second edition, published by John Willey & Sons, Inc., pp. 329- 461.

SLOPE/W (2002). Stability Analysis. Users Guide Version 5, GeoSlope Office, Canada. www.geoslope.com.

Smith, G. N. (1986). Probability and statistics in civil engineering: An introduction, Collins, London.

Smith, M. (1993). Neural networks for statistical modeling, Van Nostrand Reinhold, New York.
Spencer, E. (1967). A method of Analysis of the Stability of Embankments, Assuming Parallel Interslice Forces. Geotechnique, Vol. 17, pp. 11-26.

Stone, M. (1974). "Cross-validatory choice and assessment of statistical predictions." Journal of Royal Statistical Society, B 36, 111-147.

Twomey, J. M., and Smith, A. E. (1997). "Validation and verification." Artificial neural networks for civil engineers: Fundamentals and applications, N. Kartam, I. Flood, and J. H. Garrett, eds., ASCE, New York, 44-64.

Zaman M., Booker, J. R. and Gioda, G. (2000), Modeling in Geomechanics, John Wiley and Sons, U.K.

Zurada J. M. (1992), Introduction to Artificial Neural Systems. West Publishing Company, St. Paul, MN.

Visentini, M.1953. The latest floods of the Po River, in: Proceedings of the XVIII International Conference on Navigation.

Von Neumann J. (1958), The Computer and the Brain. New Haven, Conn.: Yale University Press, 87.

Wakai A. and Ugai K. (1999), Dynamic analyses of slopes based on a simple strain softening model of soil. Slope Stability Engineering, Yagi, Yamagami & Jiang, Balkema, Rotterdam, pp. 647-652.

Widrow B. and Hoff M .E. Jr. (I960), Adaptive Switching Circuits. 1960 IRE Western Electric Show and Convention Record, part 4 (Aug. 23): 96-104.

Wyllie, D.C. & Mah, Ch.W. 2004. Rock Slope Engineering. Civil and mining, 4th ed. Spon Press.

Yang, Y., and Rosenbaum, M. S. (2002). "The artificial neural network as a tool for assessing geotechnical properties." Geotechnical Engineering Journal, 20(2), 149-168.

Zanchettini, D., Traverso, P.& Tomasino, M. 2008. Po River discharge: a preliminary analysis of a 200-year time series, Climatic Change, 88, 411–433, DOI:10.1007/s10584-008-9395-z.

Zhang Y. J. (2001), A summary on the present advances of landslide studies. Journal of China Carsologica Sinica, Vol.18, No.3.